Title:

The Flow Convergence-Routing Hypothesis for Pool-Riffle Maintenance in Alluvial Rivers

Authors:

Michael L. MacWilliams, Jr.[1], Joseph M. Wheaton[2,3], Gregory B. Pasternack[3], Robert L. Street[1], Peter K. Kitanidis[1]

Addresses:

[1] Environmental Fluid Mechanics Laboratory, Department of Civil and Environmental Engineering, Stanford University, Stanford, CA, 94305-4020.

[2] School of Geography, University of Southampton, Highfield, Southampton, S017 1BJ, United Kingdom

[3] Department of Land, Air, and Water Resources, University of California, Davis, One Shields Avenue, Davis, CA, 95616-8626.

Keywords: velocity reversal, pool-riffle, hydrodynamics, flow convergence, numerical modeling, bed shear stress, channel morphology, river modeling

Abstract

The velocity-reversal hypothesis is commonly cited as a mechanism for the maintenance of pool-riffle morphology. Although this hypothesis is based on the magnitude of mean flow parameters, recent studies have suggested that mean parameters are not sufficient to explain the dominant processes in many pool-riffle sequences. In this study, two- and three-dimensional models are applied to simulate flow in the pool-riffle sequence on Dry Creek, CA, where the velocity reversal hypothesis was first proposed. These simulations provide an opportunity to evaluate the hydrodynamic mechanics underlying the observed reversals in near-bed and section-averaged velocity, and are used to investigate the influence of secondary currents, the advection of momentum, and cross-stream flow variability. The simulation results support the occurrence of a reversal in mean velocity and mean shear stress with increasing discharge. However, the results indicate that the effects of flow convergence due to an upstream constriction and the routing of flow through the system are more significant in influencing pool-riffle morphology than the occurrence of a mean velocity reversal. The hypothesis of flow convergence-routing is introduced as a more meaningful explanation of the mechanisms acting to maintain pool-riffle morphology.

1. Introduction

The velocity-reversal hypothesis was introduced by *Keller* [1971] as a mechanism for understanding the maintenance of pool-riffle sequences in alluvial streams. This hypothesis was based on observations from Dry Creek, California, that "at low flow the bottom velocity is less in the pool than in the adjacent riffles, and that with increasing discharge the bottom velocity in pools increases faster than in riffles" [*Keller*, 1971]. The velocity-reversal hypothesis proposes the removal of fine sediment from riffles into pools during low flows since velocity (or shear stress) is at a maximum over riffles [*Sear*, 1996]. As discharge rises, the velocity in pools increases and becomes greater than over riffles, resulting in a 'velocity reversal.' This hypothesis has initiated significant discussion in the literature and underlies a variety of conceptual models which attempt to describe the maintenance of pool-riffle morphology.

Although Keller's proposal of the hypothesis focused on mean bottom velocities, more recent studies have expanded the hypothesis to apply to mean boundary shear stress [*Lisle*, 1979], section-averaged velocity [*Keller and Florsheim*, 1993], and section-averaged shear velocity [*Carling*, 1991]. Other studies have focused on point measures of velocity and shear stress [*Petit*, 1987, 1990]. A brief synopsis of the primary studies which have addressed the velocity reversal hypothesis, including the type of study, the parameter evaluated, and our evaluation of the authors' support for the velocity reversal is given in the first three columns of Table 1. A more thorough discussion is presented in *MacWilliams* [2004].

As seen in Table 1, the literature does not provide a clear consensus or single governing hypothesis for the mechanisms controlling pool-riffle morphology. Although there has been significant debate about whether a reversal of one or more flow parameters takes place, there is more general agreement that many cross-sectional average flow parameters in pools and riffles tend to converge as discharge increases [*Carling and Wood*, 1994]. While the literature suggests that a velocity reversal does occur in some cases, it is not clear whether a reversal of some type is a requisite for pool maintenance or whether the reversal hypothesis is applicable for all pool-riffle sequences. For example, *Clifford and Richards* [1992] found that a reversal or its absence could be demonstrated simultaneously for a given pool riffle sequence depending on the parameter evaluated, and the location of the measurement or cross-section. Support for a reversal hypothesis based on reversals in different types of flow parameters (as seen in Table 1) should be considered as a suite of multiple working hypotheses for explaining pool-riffle morphology rather than a single ruling hypothesis because different maintenance mechanisms may operate in different pool-riffle sequence. However, a review of all the published field data for sediment transport in pool-riffle sequences [*Sear*, 1996] has shown that a velocity or shear stress reversal does not explain all of the published evidence of sediment transport. Thus, a more fundamental motivating question is that within systems that exhibit reversals of some kind, is the reversal an adequate explanation for pool maintenance? If not, and some alternative maintenance mechanism is hypothesized, can that alternative hypothesis explain pool maintenance in pool-riffle sequences that do not exhibit reversals?

The extension of Keller's velocity reversal hypothesis from mean bottom velocity (as it was originally proposed) to section-averaged variables has been driven in part by the use of one-dimensional models to analyze pool-riffle sequences. *Keller and Florsheim* [1993] used a one-dimensional hydraulic model (HEC-RAS) to evaluate the velocity reversal hypothesis using

Keller's original field data. They found that during high flows the mean pool velocity exceeded that of adjacent riffles, and that during low flows, the condition was reversed. Applying a similar model (HEC-2), *Carling and Wood* [1994] demonstrate the effect of varying channel width, riffle spacing, and channel roughness on the shear velocity, section mean velocity, and energy slope. However, in their results a reversal in the mean velocity took place only when the riffle was considerably wider than the pool. Similarly a 'shear velocity reversal' took place only when the pool was rougher than the riffle. Both of these conclusions severely limit the conditions when a section-averaged velocity or shear velocity reversal could potentially occur and suggest that other mechanisms may be necessary to explain sediment transport in pool-riffle sequences. *Carling* [1991] found a convergence in mean velocity in pools and riffles in his study site, but concluded that riffles were not sufficiently wide at high flows to accommodate the known discharge with a velocity lower than in pools, and thus no velocity reversal was identified. Similarly, *Richards* [1978] found a narrowing of the difference in mean depth and velocity with discharge, but neither of these variables, nor surface slope or bed shear showed any tendency to equalize at the highest flow simulated. Based on their results, *Keller and Florsheim* [1993] concluded that more sophisticated models of the hydraulics associated with pool-riffle sequences will be able to explain in more detail the interaction between channel form and process in pool-riffle sequences in alluvial streams.

There is a growing recognition that section-averaged data are not sufficient to explain the dynamics of pool-riffle sequences. Several studies have implemented two-dimensional models to simulate flow in pool-riffle sequences [e.g., *Miller* 1994; *Thompson et al.*, 1998; *Cao et al.*, 2003]. Although *Miller* [1994] focused primarily on flow around a debris fan, his results identified the influence of flow convergence at the upstream end of the fan leading to the development of scour holes; thus, his results demonstrate the importance of flow convergence in the formation of a riffle-pool sequence. Note that in this context ‘convergence’ is used to define the physical process of funneling of flow rather than in the context of a narrowing difference between mean parameter values as it was used previously. Similarly, *Thompson et al.* [1998] identified the importance of a constriction at the head of the pool at creating a jet of locally high velocities in the pool center, and the formation of a recirculating eddy. *Cao et al.* [2003] found that at low discharge there exists a primary peak zone of bed shear stress and velocity at the riffle tail in line with the maximum energy slope, and a secondary peak at the pool head. With increasing discharge, the secondary shear stress peak at the head of the pool increases and approaches or exceeds the primary shear stress peak over the riffle. They also attributed the existence of a flow reversal in their simulation to the constriction at the pool head. *Booker et al.* [2001] applied a three-dimensional CFD model to a natural pool-riffle sequence. In their study, only three out of eight possible pool-riffle couplets experienced a mean velocity reversal. They found a tendency for near-bed velocity direction to route flow away from the deepest part of pools and suggest that this flow routing may have an important influence on sediment-routing and the subsequent maintenance of pool-riffle morphology.

The velocity reversal hypothesis was proposed by *Keller* [1971] based on bed velocity measurements in a pool-riffle sequence on Dry Creek, CA. The bed-velocity data [*Keller*, 1969, 1970] support a convergence of near-bed velocity, and a reversal in near-bed velocity is predicted for higher discharges. *Keller and Florsheim’s* [1993] one-dimensional modeling study support a reversal in mean velocity for the pool-rifle sequence on Dry Creek. The overall goal of this paper is to return to Keller's original dataset to evaluate the flow processes in a pool-riffle sequence using two-dimensional and three-dimensional numerical simulations that may be able to explain the hydrodynamic mechanics underlying the observed conditions, which was not possible by previous one-dimensional simulation. Specific objectives include: 1) identifying pool-riffle "reversals" in near-bed velocity, depth-average velocity, section-average velocity, and bed shear stress; 2) evaluating the roles of secondary circulation and width constriction at the site; and 3) assessing whether the velocity reversal hypothesis is an adequate explanation for the maintenance of the pool-riffle morphology for this pool-riffle sequence. Although the study only investigates one site in detail, the fluid mechanics processes simulated in these models are transferable to other sites. Based on our analysis, a new "flow convergence-routing" hypothesis for pool-riffle maintenance in alluvial rivers is proposed, which is consistent with Dry Creek conditions and those observed other sites reported in the literature. The new hypothesis is significant for its ability to explain why past studies on other field sites have differed in their assessment of the originally proposed velocity reversal mechanism.

2. Methods

In this study, the Dry Creek reach mapped in Keller's original field study was modeled using a two-dimensional hydrodynamic model and a three-dimensional hydrodynamic model. The dual objectives of this approach were to develop a detailed evaluation of the important morphological processes that operate on this pool-riffle sequence and to evaluate the capacity of one-, two- and three-dimensional models to identify these processes. Specifically, the one-dimensional results from *Keller and Florsheim* [1993] and the results from the two- and three-dimensional models applied in this study were used to assess whether a reversal in mean velocity occurred on Dry

Creek. Further, the three-dimensional model was used to compare predicted bed velocity to the measurements from *Keller* [1971] and to evaluate whether a near-bed velocity reversal occurs, as Keller originally predicted. Lastly, the predicted bed shear stresses from the two- and three-dimensional simulations were used to evaluate whether a reversal in bed shear stress occurred and whether the spatial or temporal distribution of bed shear stresses indicate any other important mechanisms that could account for a reversal in sediment transport competence.

2.1 Two- and Three-dimensional Modeling

The two-dimensional Finite Element Surface Water Modeling System (FESWMS) was used to analyze depth-averaged hydrodynamics following the approach of *Pasternack et al.* [2004]. Three-dimensional simulations were made using the three-dimensional non-hydrostatic hydrodynamic model for free-surface flows on unstructured grids, UnTRIM, described in *Casulli and Zanolli* [2002]. The UnTRIM model was modified to include an inflow boundary condition for volume and momentum, a radiation outflow boundary condition, and a modified formulation of bed drag and vertical eddy viscosity as described in *MacWilliams* [2004]. Although the two- and three-dimensional models were applied independently, to the extent possible, the model parameters used in the two- and three-dimensional simulations were the same as the model parameters used in the one-dimensional model presented in *Keller and Florsheim* [1993], to allow for a balanced comparison between the three models.

The bathymetry for the Dry Creek field site [*Keller*, 1969] was digitized to generate a Digital Elevation Model (DEM) of the study reach in Autodesk's LandDesktop R3 Terrain Manager (Figure 1). The refined DEM data was then exported and interpolated onto each of the model grids. The total reach modeled is approximately 135 m long and ranges in width from 20 and 25 m. The FESWMS model used a finite element mesh with an approximately uniform node spacing of 0.45 m. This resulted in a model mesh with roughly 12,600 computational nodes comprising approximately 3500 mixed quadrilateral and triangular elements. For the UnTRIM model, an unstructured horizontal grid consisting of 23,655 cells was developed using TRIANGLE [*Shewchuk*, 1996]. The average grid cell size was 0.12 m^2. The seven cross-sections in the study reach (Figure 1) were preserved in the model grids by aligning the edges of the model grid cells along the section lines. This facilitated direct comparison of model results with Keller's field data at specific cross-sections. A uniform vertical grid spacing of 0.05 m was used for the UnTRIM simulations.

A detailed mapping of roughness for the Dry Creek site was not available. However, *Keller's* [1969] field data on grain size variations within the site suggest that such roughness variations are minor. Further, *Keller and Florsheim* [1993] showed that hydraulic model results were not sensitive to these very small variations in roughness parameterization. Thus, a constant roughness parameter was applied in both the FESWMS and the UnTRIM simulations. In the FESWMS simulations the Manning's *n* roughness was estimated as 0.041 for entire study site. For the UnTRIM simulations a constant z_o roughness of 1.5×10^{-3} m was applied. Based on the method described in *MacWilliams* [2004], this roughness height corresponds to a Manning's *n* value of approximately 0.041 for the range of flow depths simulated.

For the FESWMS simulations, Boussinesq's analogy was applied to parameterize eddy viscosity, which crudely approximates eddy viscosity as an isotropic scalar. Doing so allows a theoretical estimate of eddy viscosity as 60 percent of the product of shear-velocity and depth [*Froehlich*, 1989]. A constant eddy viscosity value of 0.027 m^2/sec was used for all FESWMS model runs. It is well known that the eddy viscosity has a nearly parabolic distribution with depth in an open channel flow and that the use of a constant eddy viscosity for three-dimensional simulations is likely to yield unrealistic vertical velocity profiles [*Rodi*, 1993]. As a result, in uniform open channels, the velocity profile is often assumed to be parabolic, resulting in a parabolic eddy viscosity distribution [*Celik and Rodi*, 1988]. For the UnTRIM simulations, a parabolic vertical eddy viscosity model was applied following the approach of *Celik and Rodi* [1988].

Keller's original field measurements [*Keller*, 1969, 1971] were made at discharges of 0.42, 0.97, and 4.5 m^3/s. The HEC-RAS model simulations by *Keller and Florsheim* [1993] were conducted for five steady flow rates, including the three discharges measured by *Keller* [1969] and two larger discharges of 8.5 and 17 m^3/s. These five flow rates were modeled as five separate steady flow simulations in FESWMS; in UnTRIM a transient simulation of each flow rate was run until the flow field reached a 'steady state.' In both UnTRIM and FESWMS, the inflow discharge was specified at the upstream end of the channel; at the downstream end of the channel, the elevation was specified based on the elevations predicted at the downstream cross-section from the modeled results of *Keller and Florsheim* [1993]. To allow direct comparison with previous studies, we evaluated the model results at the pool cross-section (Section 19, Figure 1) and riffle cross-section (Section 21, Figure 1) used in the analysis of *Keller* [1971] and *Keller and Florsheim* [1993].

2.2 Bed Velocity

Based on bed velocity measurements on Dry Creek, *Keller* [1971] predicted the occurrence of a bed velocity reversal. *Keller* [1969] believed that the "bottom velocity is much more significant in analyzing bed-load movement than the mean velocity of the entire stream." Keller collected velocity measurements near the bed and at 0.6 times the depth at three foot intervals along each of four cross-sections during measured discharges of 0.42, 0.97, and 4.5 m^3/s. Velocities near the bed were measured with at rod-mounted, pigmy Price current meter [*Keller*, 1970]. For comparison with the bottom velocity measured by Keller, the velocity predicted using UnTRIM in the bottom two cells in each water column was interpolated to estimate the average velocity at a depth of 5 cm. Based on the geometry of the instrument used, this seems to be a reasonable estimate of the lowest height at which the velocity could feasibly be sampled. Because the pigmy Price current meter method does not measure flow direction and assumes all flow is in one direction, the overall velocity magnitude predicted by UnTRIM is used rather than only the downstream flow component. This distinction is significant for areas in which significant secondary circulation exists near the channel bed. Comparisons of bed velocity were not made using the FESWMS results, since FESWMS is a depth-averaged model.

2.3 Section-Averaged Velocity

Keller and Florsheim [1993] extended *Keller's* [1969] original proposal of a reversal in bed velocity to a reversal in mean cross-section velocity. In their analysis, the field measurements from *Keller* [1969] were averaged over the pool and riffle cross-sections and HEC-RAS was used to model section-averaged velocity. In this study, the predicted flow fields from FESWMS and UnTRIM at the pool and riffle cross-sections were also averaged at the pool and riffle cross-sections to obtain the cross-sectional average velocities for each of the five flow rates. These average velocities were compared to the results presented by *Keller and Florsheim* [1993].

2.4 Bed Shear Stress

The predicted bed shear stress was calculated over the model domain for both the UnTRIM and FESWMS simulations. For the FESWMS simulations, the depth-average shear stress was calculated from depth, velocity, and bed roughness using a drag force relation [*Froehlich*, 1989]. Bed shear stress for the FESWMS simulation was calculated as 0.51 times the depth-average shear stress based on a detailed validation study (*Pasternack et al.*, submitted for publication, 2005). In the UnTRIM simulations, the bed shear stress was calculated from the near-bed velocity by assuming a log-law near the bed [*MacWilliams*, 2004].

3. Results

The predicted downstream velocities from the UnTRIM simulation at the pool cross-section are shown in Figure 2. The highest velocities occur near the surface, and the flow tends to be concentrated in the center section of the pool, with the highest velocities near the bed occurring over the point bar side of the pool rather than in the deepest section of the pool. This effect becomes more pronounced at higher discharges. The predicted surface velocity and flow depth for the 0.42 and 17.0 m^3/s discharges are shown in Figure 3. At a discharge of 0.42 m^3/s the highest surface velocities are predicted over the riffle upstream of the pool cross-section and over the riffle cross-section. There is little variation of surface velocity across the pool cross-section. At a discharge of 17.0 m^3/s, there is a noticeable funneling of surface velocities over both the pool and the riffle cross-sections, such that the highest predicted surface velocities at the pool cross-section occur within a narrow zone. At the pool cross-section, low surface velocities are predicted in the shallower areas on the point bar. As seen in Figure 3, the pool cross-section widens more with discharge than the riffle cross-section; the shallow channel margins on the riffle cross-section are much smaller than on the pool cross-section.

3.1 Bed Velocity

The bed velocity measurements at the pool and riffle cross-sections are compared with the predicted near-bed velocity from UnTRIM on Figures 4 and 5, respectively. There is generally good agreement between the measured bed velocity and the bed velocity predicted by UnTRIM at the pool cross-section for each of the three discharges at which data was collected (Figure 4). No data were collected in the deepest part of the pool for the 4.5 m^3/s flow rate because the water was too deep and swift to collect measurements (*Keller*, unpublished field notebook, 1969). At all three discharges, the maximum measured and maximum predicted bed velocity at the pool cross-section does not occur in the deepest part of the pool.

For the riffle cross-section, shown in Figure 5, there is also very good agreement between the measured and modeled bed velocity for each of the three discharges at which data was collected. The biggest observed difference between the field observations and the model predictions occurs on the right margin of the riffle cross-section for a discharge of 4.5 m^3/s. As will be discussed below, this area of the riffle cross-section exhibits significant secondary circulation at a discharge of 4.5 m^3/s and higher; for these discharges the predicted cross-stream velocity component near the bed is of a comparable magnitude to the downstream velocity component in this portion of the riffle. This flow complexity, and any unsteadiness associated with these flow patterns, appears to be the primary mechanism responsible for the difference between the predicted and observed bed velocity on the right edge of the riffle cross-section. However, overall the simulation results show good agreement with the field observations at the riffle cross-section. The agreement between the predicted and measured bed velocity at both the pool and riffle sections for the three discharges at which data is available indicates that the UnTRIM model is accurately simulating flow in Dry Creek at these discharges.

3.2 Section-Averaged Velocity

The predicted cross-sectional average velocities at the pool and riffle cross-sections are shown as a function of discharge in Figure 6. For all flows, the HEC-RAS model [*Keller and Florsheim*, 1993] predicted a somewhat lower mean velocity (larger cross-sectional area) at the riffle cross-section than the 2-D and 3-D models, with the largest differences occurring for the lower discharges. The 2-D and 3-D models show better agreement with the field data for the riffle cross-section. All three models show reasonably good agreement with the field data [*Keller*, 1969] at the pool cross-section for the three discharges at which data was collected. Using HEC-RAS, *Keller and Florsheim* [1993] predicted a reversal in mean velocity at approximately 3.3 m^3/s. The FESWMS (2-D) simulation predicts a reversal in cross-sectional average velocity at approximately 5.9 m^3/s, and the UnTRIM (3-D) simulation results predict a reversal in mean cross-sectional velocity at a discharge of approximately 3.8 m^3/s. In this context, a reversal refers to the discharge at which the cross-sectional average velocity at the pool cross-section exceeds the cross-sectional average velocity at the riffle cross-section. Because the instantaneous discharge in both cross-sections is identical, a reversal in mean cross-section velocity corresponds identically with a reversal in mean cross-sectional area. This reversal in cross-section area is largely a function of the site geometry, as discussed below. However, this analysis shows that all three models predict a reversal in cross-sectional average velocity for this pool-riffle sequence on Dry Creek.

3.3 Bed Shear Stress

Planform maps of bed shear stress for four of the five discharges simulated from the UnTRIM and FESWMS simulations are shown in Figures 7 and 8, respectively. For the 0.97 m^3/s flow (Figures 7a, 8a) the UnTRIM and FESWMS simulations predict a similar distribution of shear stress, with the highest shear stresses occurring over the upstream riffle and a narrower zone of high shear stresses through the pool cross-section which widens downstream over the riffle cross-section. This zone of higher shear stress along the center of the channel becomes more pronounced with increasing discharge. The UnTRIM simulations predict a more distinct band of higher shear stresses along the center of the channel with lower shear stresses along the channel margins (and in the deepest part of the pool). The shear stress distribution predicted by the FESWMS simulations shows a more uniform distribution of shear stresses across the channel, but still show the highest shear stresses concentrated in the center of the channel. As with the near-bed velocity (Figure 4), the maximum bed shear stresses predicted at the pool cross-section occur on the slope of the point bar, rather than in the deepest part of the pool for both models and at all discharges. At the riffle cross-section, the bed shear stress at the lower two flow rates is fairly uniform across the channel, with the highest values occurring near the middle of the cross-section and at a local topographic high point (e.g., Figure 11a). In general, the bed shear stresses predicted from the FESWMS simulations (Figure 8) tend to be slightly higher than the bed shear stresses predicted from the 3-D UnTRIM simulations (Figure 7). This discrepancy results from calculating the bed shear stress from the depth-averaged velocity rather than the near-bed velocity.

The bed shear stresses shown in Figure 7 were averaged over the pool and rifle cross-sections. Figure 9 shows the cross-sectional average and cross-section maximum shear stresses at the pool and riffle cross-sections predicted using UnTRIM. The shear stress predicted by applying the slope depth product at the pool and riffle cross-sections is also shown for comparison. A reversal in cross-sectional averaged bed shear stress occurs at a discharge of 3.0 m^3/s and a reversal in maximum cross-section bed shear stress occurs at a discharge of 3.9 m^3/s. The shear stresses predicted using the depth-slope product show a reversal at a discharge of 0.94 m^3/s.

3.4 Secondary Circulation

Although the analysis of cross-sectional average parameters provides a relatively simple metric for analyzing flow processes, cross-sectional average parameters do not reliably account for flow complexity in systems where significant secondary circulation exists. Figure 10 shows the magnitude and direction of flow component perpendicular to the downstream flow direction at the pool cross-section for four of the five discharges studied. As seen in this figure, significant secondary circulation cells develop at the pool cross-section for the discharges of 4.5 m^3/s and greater. The degree of secondary circulation predicted at the pool cross-section increases significantly with discharge. At the 0.42 (not shown) and 0.97 m^3/s flow rates, a single small secondary circulation cell is visible in the deepest part of the pool. As the discharge increases, the velocity magnitude of the circulation cells increases significantly and a separate weaker circulation cell develops over the shallow section of the point bar. These results are consistent with field observations made by Keller at the Dry Creek site. His field observations suggest there is considerably more turbulence at high flows in pools than in adjacent point bars and that some pools in Dry Creek appear to be formed by "vertical vortexes" scouring the pool bottom [*Keller*, 1969]. By "vertical vortices" it is assumed that Keller is referring to the large vertical circulation cells visible in Figure 10 at higher discharges. These circulation cells are also likely to play a significant role in mobilizing sediments in the deepest portion of the pool as discharge increases. It should also be noted that in general the secondary flow at the pool-cross-section shows a dominant flow direction from left to right. This tendency becomes more pronounced as discharge increases, especially near the surface over the point bar where the downstream velocities are largest. This effect indicates that the cross-section line is not exactly perpendicular to the primary flow direction (cross-section location on Figure 1; flow direction on Figure 3). However, since this cross-section alignment was used by *Keller* [1969, 1971] and *Keller and Florsheim* [1993], this alignment is maintained in this study. Figure 11 shows the magnitude and direction of flow component perpendicular to the downstream flow direction at the riffle cross-section for four of the five discharges studied. At the 0.97 m^3/s discharge, a small circulation cell is visible on the right side of the cross-section. The magnitude of this circulation cell increases significantly with increasing discharge. A second weaker eddy is visible on the left side of the cross-section for discharges of 4.5 m^3/s and greater.

4. Discussion

4.1 Bed Velocity

Keller's original bed velocity measurements showed a convergence rather than a reversal in mean bed velocity; however, *Keller* [1969, 1971] postulated that a reversal in mean bed velocity would occur at a discharge above 4.5 m^3/s. By averaging the near-bed velocity at the pool and riffle cross-sections for each of the five flow rates, it is possible to determine whether a reversal in mean near-bed velocity occurs in Dry Creek. The UnTRIM simulations predict a reversal in mean cross-section bed velocity at approximately 4.0 m^3/s and a reversal in maximum cross-section bed velocity at approximately 5.1 m^3/s. The consideration of the maximum bed velocity is significant because it is the locally maximum bed velocity in the cross-section rather than the cross-sectional average value which gives a better indication of the local sediment transport competence. A reversal in mean bed velocity occurred prior to a reversal in maximum bed velocity, while the predicted reversal in mean bed velocity occurred at a slightly lower discharge than was predicted by *Keller* [1971]. However, these results support *Keller's* [1971] original prediction that a reversal in near-bed velocity would occur on his pool-riffle study site on Dry Creek.

4.2 Section-Averaged Velocity

Through a systematic modeling study using a 1-D model, *Carling and Wood* [1994] found that a reversal in mean cross-section velocity only took place when the riffle was considerably wider than the pool. At the Dry Creek field site, the riffle is approximately 50% wider than the pool at a flow rate of 0.42 m^3/s, 25% wider than the pool at a flow rate of 4.5 m^3/s, and slightly narrower than the pool at a discharge of 17.0 m^3/s (e.g., Figure 7). The widening of the pool at a higher rate with increasing discharge appears to be one of the controlling geometric factors required for a reversal in section-averaged velocity; this condition is met on Dry Creek based on both the one-dimensional modeling results of *Keller and Florsheim* [1993] and the two- and three-dimensional modeling presented in this study predict a reversal in mean velocity (Figure 6).

4.3 Bed Shear Stress

Carling and Wood [1994] found that a 'shear velocity reversal' took place whenever the pool was rougher than the riffle, but under no other conditions. In their study, the shear velocity was calculated as $U_* = \sqrt{gdS}$, where g is gravity, d is the average water depth, and S is the energy slope. Based on this equation, commonly referred to as the depth-slope product, a higher value of the shear velocity is highly dependant on the energy slope. The average cross-sectional depth and water surface slope (as a proxy for energy slope) predicted at the pool and riffle cross-sections from the UnTRIM simulations were used to calculate the shear velocity using this equation. The simulation results showed a significant variation in water surface elevation and downstream water surface slope along the cross-section, making the calculation of a meaningful cross-sectional average energy slope difficult. As a result, the average water surface slope was calculated over a 10 m reach centered on the pool and riffle cross-sections. The average depth of the riffle was less than the average depth of the pool for the discharges less than 17.0 m^3/s, but greater than the average depth of the pool for a discharge of 17.0 m^3/s. This reversal in average depth occurs due to the widening of the pool onto the shallow areas of the point bar with increasing discharge (seen in Figure 3), whereas the riffle width does not increase as significantly with discharge. At the riffle cross-section, the increase in flow depth with discharge is more pronounced than the increase in width. The water surface slope at the riffle cross-section decreases with discharge; the water surface at the pool cross-section steepens with discharge for the first three discharges and then decreases in slope for higher discharges. The difficulty associated with calculating a representative average water surface slope increases with discharge because the water surface elevation along and across the cross-section becomes more complex at higher discharges. Thus, there is a significant degree of uncertainty in the estimates of water surface slope at higher discharges. Applying the average depth and water surface slope parameters to the above equation predicts a reversal in bed shear stress at a discharge of 0.94 m^3/s. This result is not consistent with the predicted mean and maximum bed shear stresses shown in Figure 9. Similarly, the shear stress maps shown on Figure 7 and 8 do not support the drop in shear stress at the pool and riffle cross-sections for the highest discharge, as is predicted by the application of the depth-slope product.

This analysis of shear velocity using a one-dimensional approach illustrates the inappropriateness of applying one-dimensional equations to flows where significant cross-stream flow patterns are evident. In flows where significant two- and three-dimensional flow patterns are significant, one-dimensional step-backwater models (such as HEC-RAS) do not provide a reliable estimate of friction slope and the slope-depth product does not yield a reliable estimate of shear velocity. *Thompson et al.* [1996] have argued that water surface slope is of little use in the calculation of shear stresses in systems where complex wave patterns and localized flow conditions influence longitudinal water-surface slopes. In addition, variations in water-surface elevation along a given cross-section also lead to a range of possible water-surface slopes between two given cross-sections [*Miller*, 1994]. These factors all suggest that a one-dimensional approach is not appropriate for estimating bed shear stress in this pool-riffle sequence.

A comparison of the predicted shear stresses from the FESWMS and UnTRIM simulations (Figures 7 and 8) provides insight into the relative importance of three-dimensional flow processes on predicting bed shear stress on Dry Creek. As mentioned above, one of the important mechanisms identified by the UnTRIM simulation is the convergence of the highest shear stresses into a narrow zone of flow routing through the channel. A qualitative comparison of Figures 7 and 8 shows that the width of higher shear stresses relative to the overall width of the channel is much narrower in the UnTRIM simulation than the FESWMS simulations. Part of this difference results because the secondary circulation cells on both margins of the channel (Figure 10 and 11) act to enhance the concentration of the flow in the center of the channel. Additionally the use of a horizontal eddy diffusivity in the FESWMS model acts to smooth out the horizontal velocity gradients, thereby reducing cross-stream flow variability. These conclusions are supported by additional 2-D simulations made using UnTRIM which show less flow convergence than the 3-D UnTRIM simulations, but more flow convergence than the FESWMS simulations.

4.4 Secondary Circulation

Clifford and Richards [1992] have argued that "the interaction between channel form at any point within a riffle-pool unit depends in part on flow and sediment behavior in upstream and downstream units," and that "if anything, explanations relying on cross-sectional averages complicate, rather than clarify, the characteristics of flow and form interaction." *Clifford and Richards* [1992] base this argument in part on the difficulty in accurately calculating the energy slope in the presence of complex secondary flow, and conclude that in the presence of a complex secondary flow the application of a 1-D equation of the form of equation discussed above is unacceptable. The results presented in the previous section, which demonstrate the significant secondary circulation patterns at both the pool and riffle cross-sections, and the apparent inconsistencies found when applying the depth-slope equation to the range of flows simulated on Dry Creek, support this conclusion.

4.5 Flow Constriction

Thompson et al. [1996, 1998] have revised the traditional velocity reversal model to incorporate the effects of a channel constriction at the head of a pool. Their study demonstrated how the upstream constriction resulted in higher local velocities in the pool in comparison to adjacent riffles, despite a similar cross-sectional area. This effect is also observed in the predicted velocities at the pool and riffle cross-sections on Dry Creek. As noted by *Booker et al.* [2001], this concept links the concept of velocity-reversal with work by *Keller* [1972] which suggested that the regular pattern of scour and deposition required for pools and riffles may be provided by an alternation of convergent and divergent flow patterns along the channel. This connection is significant because the pool-riffle sequence on Dry Creek also has a constriction at the head of the pool.

Keller [1969] found that the at-a-point maximum bottom velocities at the pool cross-section (Figure 4) showed a tendency for the highest velocities to be located on the point bar side of the pool rather than in the center of the pool. His bottom velocity measurements suggest that the area of high bottom velocity is “never in the center of the pool” and that “with increasing velocity there is a tendency for the area of high bottom velocity to migrate toward the point bar side of the pool” [*Keller*, 1969]. This feature is also observed in the shear stress distribution predicted by the UnTRIM simulations shown in Figure 7. The highest near-bed velocities, and thus the highest bed shear stresses, occur on the point bar and not in the deepest part of the pool. The alignment of this area of high flow velocity and shear stress with the flow constriction upstream of the pool on Dry Creek suggest that the upstream flow constriction is playing an important role in flow routing through the pool cross-section.

To test the influence of the upstream constriction on the velocity and shear stress distribution in the pool cross-section on Dry Creek, an additional UnTRIM simulation was made with a modified numerical method that neglects the advective acceleration terms in the three-dimensional model. In effect, this approach removes any potential effects resulting from the flow convergence associated with the constriction at the head of the pool. The velocity distribution at the pool cross-section for the simulation which neglects advective acceleration, shown in Figure 12, shows a dramatically different velocity distribution than was observed in the simulation results shown in Figure 2. For the simulation without advective acceleration, the maximum velocities and shear stresses occur over the deepest part of the pool instead of over the point bar as was observed by *Keller* [1969] and seen in the simulation results presented in the previous section. This result shows that the constriction at the head of the pool on Dry Creek is having a significant impact on the hydrodynamics of the pool-riffle sequence on Dry Creek. It also demonstrates that models that do not incorporate the full complexity of three-dimensional hydrodynamics and advective acceleration can not accurately predict the important flow processes that occur in the pool-riffle sequence on Dry Creek. This result supports the results of *Whiting and Deitrich* [1991] which show that convective acceleration terms are important where topographic forcing leads to significant cross- and downstream flow accelerations. Another interesting outcome of this simulation without advective acceleration is that the results still predict a reversal in mean velocity at a discharge of 4.5 m^3/s. This result supports the conclusion that the occurrence of a mean velocity reversal is controlled more by the geometry of the site than by the dominant flow processes in the pool-riffle sequence.

Several recent modeling studies have also identified the influence of constrictions in influencing pool-riffle morphology. *Cao et al.* [2003] conclude that a channel constriction can, but may not necessarily, lead to [sediment transport] competence reversal, depending on channel geometry, flow discharge, and sediment properties. *Booker et al.* [2001] conclude that an analysis of near-bed velocity patterns suggested that the near-bed flow direction can cause routing of sediments away from the deepest part of the pools. Their results indicate maintenance of pool-riffle morphology by a lack of sediment being routed into pools rather than an increased ability to erode based on convergence of flow into the pool. This process also appears to be playing a dominant role in Dry Creek since the convergence of flow caused by the constriction may act to route sediment across the point bar, instead of through the deepest part of the pool.

4.6 Flow-Convergence Routing

Clifford and Richards [1992] concluded that there is a need to formulate explanations of the maintenance of pool-riffle sequences that are sensitive to local variation and the existence of spatially distributed form-process feedbacks. The results of the three-dimensional simulations of the pool-riffle sequence on Dry Creek support this conclusion. While the simulation results support a reversal in mean velocity, mean bed velocity, mean bed shear stress, and a variety of other cross-sectional average parameters, the results indicate that the occurrence of a reversal in mean parameters is not sufficient to explain the important processes that are occurring on the pool-riffle sequence on Dry Creek. The prediction of a reversal of mean velocity in the simulation without advective acceleration shows that a reversal in mean velocity is not, in and of itself, sufficient to explain the important mechanisms occurring in the pool-riffle sequence on Dry Creek. A reversal in mean velocity does not explain the occurrence of the high velocities observed on the point bar rather than in the deepest part of the pool and it does not explain the important effects that advective acceleration have on the distribution of predicted velocities in the pool cross-section. Previous studies [e.g., *Carling and Wood*, 1994] have recognized that the occurrence of a reversal in mean velocity depends on specific geometric constraints where the riffle is significantly wider than the pool. Other studies [e.g., *Richards*, 1978; *Carling*, 1991] indicated pool-riffle geometries where this condition was not met and a convergence in mean velocity rather than a reversal was predicted. Further, there is no special significance to cross-sectional average parameters which require a reversal in mean parameters to occur. While a velocity reversal, or a convergence of cross-sectional average flow parameter values is observed in many pool-riffle sequences, there is a significant body of evidence in the literature that suggests that more complicated flow processes are significant in the maintenance of pool-riffle morphology. The flow complexity evident in almost all field studies and every two- and three-dimensional modeling study of pool-riffle sequences to date indicate that one-dimensional parameters and one-dimensional models are not adequate to capture the flow complexity in pool-riffle sequences. As a result, it is a reasonable conclusion that a hypothesis for pool-riffle morphology based on cross-sectional average parameters is not appropriate for explaining all of the processes important for maintaining pool-riffle morphology.

A working hypothesis for defining the important processes for maintaining pool-riffle morphology can be introduced based on the processes observed on Dry Creek. It is called here the hypothesis of 'flow convergence-routing' and is thought to be a more meaningful mechanism for explaining the processes that are of preeminent importance in defining pool-riffle morphology in Dry Creek than the occurrence of a velocity reversal. The hypothesis draws on elements of the work of *Booker et al.* [2001] and *Thompson et al.* [1996, 1998], but elaborates about the maintenance mechanisms more explicitly. Under this hypothesis, the formation and maintenance of a pool depends on the occurrence of an upstream flow constriction which results in a convergence and acceleration of flow at the head a pool; this effectively generates a jet of flow through and downstream of the constriction. The effect of this convergence increases with discharge, and results in the development of a zone of high velocity and shear stress along a well-defined zone within the channel. Near bed flow is routed through this zone of high velocity resulting in high shear stress; this zone of high velocity and shear stress is the primary pathway for sediment movement through the pool. This zone of flow routing corresponds to the highest near-bed velocities, shear stresses, and maximum particle size. This zone is the primary pathway for sediment routing through the pool and can serve to route the coarsest sediment away from the deepest part of the pool. The lateral variation of flow along the edge of the convergence zone creates a lateral shear between the faster moving water over the point bar and the slower moving water over the deeper portion of the pool. This lateral shear zone has a significant impact on the secondary circulation pattern observed at the pool cross-section, and this circulation plays a role in mobilizing sediment in the deepest part of the pool. Depending on the geometry of the site, a separation zone and recirculating eddy may also develop. At the tail of the pool, the flow diverges at the head of the riffle leading to deposition on the riffle and the maintenance of a topographic high at the tail of the pool. This hypothesis of flow convergence-routing can explain the important processes that are evident in Dry Creek, is supported by the data and observations of *Keller* [1969], and is supported by the results of other studies of pool-riffle sequences.

A conceptual model of the flow convergence-routing mechanism during high flows on Dry Creek is shown in Figure 13. At the upstream riffle, the flow is fairly uniform across the channel. The point bar at the pool cross-section acts as a constriction, and the flow is concentrated over a smaller width of channel. This funneling of flow results in a zone of higher velocity and sediment transport competence (depicted by wide dark arrow) that acts to route flow and sediment through the pool reach. Downstream of the point bar, the flow diverges and spreads out over the downstream riffle. At a sufficient distance downstream of the constriction, the flow on the downstream riffle is again fairly uniformly distributed across the riffle.

The introduction of the flow convergence-routing hypothesis is not a rejection of the results of *Keller* [1969, 1971]. Rather, the introduction of a more detailed hypothesis is a recognition that cross-sectional average parameters are not sufficient to explain the important processes in maintaining pool-riffle morphology. However, *Keller* [1969] also identified the significance of flow convergence-routing on Dry Creek. He observed that "the point bar, which is slightly upstream, also tends to converge water into the pool. This is not significant at low flow, but may be important in producing fast bottom velocities at high flow. Water coming out of the pool diverges on the riffle, and this is probably responsible for the slower bottom velocity in the riffle at high flow." Further, Keller concluded that "it is assumed that at high flow the convergence of the pool produces fast bottom velocity which has a jetting action on the bed material; when the material reaches the divergent and slower bottom velocity of the riffle, the coarser material may be dropped from the moving traction load."

The occurrence of flow routing in Dry Creek is also supported by Keller's observations that the highest velocities in the pool tended to be located on the point bar side of the pool rather than in the center of the pool. The bedload movement experiments on Dry Creek reported by *Keller* [1969, 1970] found that 35 percent of the variability of the distance a bed-load particle will move at the field site can be explained by the variability of the bottom velocity in the vicinity of the particle, and 68 percent can be explained by the combination of velocity and particle parameters. Keller found that on riffles movement was most influenced by differences in bottom velocity. However, particle parameters—i.e., volume, weight in water, specific gravity, and shape—are considerably more important than velocity for the movement of particles through pools. Because, velocity tends to be more uniform over the riffle, the bed velocity shows a high correlation with movement over the riffles. However at the pool cross-section, two important sediment transport mechanisms occur. In the convergence zone where the near-bed velocities are highest, the significance of locally high bed velocity and shear stress is likely to be important. However, in the deeper part of the pool where bed velocities are much lower sediment mobilization is likely to rely on mobilization due to secondary circulation driven processes. In these areas, particle parameters are likely to be more significant than downstream bed shear stress as an indicator for particle movement. As seen in Figure 10, the near-bed cross-stream velocity in the deepest part of the pool is likely to exhibit lift and shear forces on the bed particles in the deeper part of the pool. The outward gravitational component acting on a particle is proportional to the cube of the grain diameter, whereas the fluid drag is proportional to the diameter squared [*Dietrich*, 1987].

Hence for the same near-bed velocity, large particles will tend to roll outward against the inward flow and smaller ones will be carried inward towards the shallow water [*Dietrich*, 1987]. This provides a mechanism whereby the fine sediments in the deepest part of the pool can be mobilized and carried into the zone of convergence where it can be transported downstream, and supports *Keller's* [1970] results that particle parameters are more significant indicators of particle mobility in pools than in riffles.

Keller [1969] reports that on Dry Creek bed material is significantly larger on bars and riffles than in the deeper parts of pools. In addition, Keller found that the large material on the point bar gradually decreases in size across the stream to the bottom of the pool. Figure 14 shows the lateral sorting of largest bed material for the pool and riffle cross-sections. There is a significant peak in largest bed material at a distance of approximately 15 m. This peak in the size of the largest bed material on both the pool and riffle cross-sections corresponds to the zone of maximum shear stress which is visible on Figure 7 at the higher discharges. This peak in coarsest bed material corresponds to the zone of flow convergence and supports the hypothesis that the largest bed materials are being routed around the deepest part of the pool rather than through it. This routing of sediment around the deepest part of the pools rather than through them resolves the paradox of why coarse sediment is not left in the pool on the receding discharge.

The hypothesis of flow convergence-routing provides an important link with the work of *Dietrich et al.* [1979] on flow and sediment transport in meandering systems. *Dietrich et al.* [1979] found that the zone of maximum boundary shear stress is near the inside bank in the upstream bend (rather than in the deeper outside portion of the pool) and then crosses the outside bank as it enters the central segment of the bend. Similarly, the downstream velocity distribution at the upstream bend presented by *Dietrich et al.* [1979] shows a similar distribution to that predicted for the pool cross-section on Dry Creek such that the highest velocities occur over the point bar rather than the deeper part of the pool on the outside bend. *Dietrich et al.* [1979] also identified a zone of maximum sediment transport corresponding to the zone of maximum boundary shear stress and the zone of maximum particle size. This zone of coarse sediment shows a similar effect of flow convergence and sediment routing over a distinct band as is observed in the sediment distribution shown in Figure 14. As seen in Figure 7, the UnTRIM simulations predict a narrow band of high shear stress which develops downstream of the constriction at the head of the pool. The predicted shear stress distributions at discharges of 4.5 and 8.5 m^3/s show a well developed zone of high shear stress along the zone of flow convergence. At the highest discharge simulated, 17.0 m^3/s, this zone of convergence is somewhat less pronounced. As seen in Figure 7, the overall flow width at the highest discharge is more uniform and the constriction is less pronounced. This suggests that the constriction may be sufficiently submerged at this discharge and therefore it does not have as significant of an influence on flow through the pool-riffle unit as it did at lower discharges.

Although the hypothesis of flow convergence-routing is introduced based on the processes observed on Dry Creek, this hypothesis is consistent with observations of the significance of flow constrictions observed in other studies of pool-riffle sequences on alluvial streams [e.g., *Thompson et al.*,1998; *Booker et al.*, 2001; *Cao et al.*, 2003]. As seen in Table 1, many of the primary references pertaining to the velocity reversal hypothesis offer either stated or implied support for the hypothesis of flow convergence-routing, since flow constrictions and flow convergence has been discussed in many of these references. The majority of the studies which do not directly support the flow convergence-routing hypothesis are one-dimensional modeling studies, which can not evaluate this mechanism.

The mechanism of flow constriction and routing observed in Dry Creek is somewhat different than the mechanism proposed by *Thompson et al.* [1996, 1998]. At their field site, *Thompson et al.* [1996, 1998] identify a constriction that blocks a portion of the channel rather than the more subtle narrowing constriction on Dry Creek. Because the channel width immediately opens up downstream of their constriction, *Thompson et al.* [1996, 1998] identify a separation zone and a recirculating eddy that form downstream of the constriction, while the primary flow is funneled into the deepest part of the pool. Although the geometry is somewhat different, the field site *Thompson et al.* [1996] also can be explained by the hypothesis of flow convergence-routing. However, in their case the flow is diverted through rather than around the deepest part of the pool. For this geometry, the flow-convergence routing mechanism is consistent with their observations that the coarsest materials found in the pool unit are in the deepest part of the pool. *Booker et al.* [2001] identify flow routing around the deepest section of the pool for all of the pool units studied, which is identical to the flow routing observed on Dry Creek. Further, *Booker et al.* [2001] note that a recirculating eddy forms in only one of their pool units, and they suggest that the presence of recirculating zones at the pool head is a phenomenon that may act to maintain pool morphology but is of secondary importance in comparison to sediment routing. This suggests that the process of flow constriction is likely to be a more prominent feature in a composite hypothesis for pool-riffle morphology than the presence of a recirculating eddy. Further consideration of the hypothesis of flow convergence-routing on additional field sites is likely to yield insight into the relative importance of each of these processes on the maintenance of pool-riffle morphology in alluvial rivers.

5. Conclusions

Two- and three-dimensional simulations of flow in the pool-riffle sequence on Dry Creek, CA are presented. The predicted flow velocities agree well with measured bed velocities by *Keller* [1969] and with average velocities predicted by *Keller and Florsheim* [1993] using a one-dimensional model. The model results show a reversal in mean velocity, mean near-bed velocity, maximum near-bed velocity, mean bed shear stress, and maximum bed shear stress in the pool-riffle sequence at discharges between 3.0 and 6.8 m^3/s. These results agree well with previous predictions of a reversal of bed velocity by *Keller* [1971] and a reversal in mean velocity by *Keller and Florsheim* [1993]. The application of the UnTRIM and FESWMS models to the Dry Creek pool-riffle sequence is significant because this field site served as the basis for the introduction of the velocity reversal hypothesis for pool-riffle sequences.

The results of both the two-dimensional and three-dimensional simulations demonstrate that the presence of a flow constriction at the head of the pool results in a flow convergence that causes the maximum velocities to occur on the point bar of the pool rather than in the deepest part of the pool. The three-dimensional model shows a greater degree of flow and shear stress convergence and further reveals that this flow convergence drives a significant secondary circulation cell in the deepest part of the pool. It is believed that flow convergence serves to route sediment across the point bar rather than through the deepest part of the pool, while secondary circulation in the pool cross-section has the potential to cause mobilization of the fine sediments in the deepest part of the pool.

Though the pool-riffle sequence on Dry Creek does experience a reversal in cross-sectional average and near-bed parameters, the results presented in this study suggest that the velocity reversal hypothesis does not explain the primary mechanisms for maintaining pool-riffle morphology on Dry Creek. In light of these results that show that non-uniform flow effects are important in driving flow and sediment routing processes in the pool-riffle sequence, the velocity-reversal hypothesis, which is based on cross-sectional average values, does not seem to be an adequate hypothesis to explain the important processes in maintaining pool-riffle morphology at this site. Although many studies of pool-riffle sequences have shown a convergence in mean parameters at pools and riffles, there is no evidence to suggest that a reversal in velocity must occur, and in fact many studies have shown that reversals do not occur at all pool-riffle sequences. For a hypothesis to be meaningful it must be able to explain the dominant processes; the velocity-reversal hypothesis does not meet this criteria.

Based on the processes observed on Dry Creek, the hypothesis of flow convergence-routing is introduced as a new working hypothesis for defining the important processes for maintaining pool-riffle morphology in alluvial rivers. Under this hypothesis, the formation and maintenance of a pool depends on the occurrence of an upstream flow constriction which results in a convergence and acceleration of flow at the head of a pool. Flow through the pool is routed through a narrow zone within the cross-section. This zone of flow routing corresponds to the highest near-bed velocities, shear stresses, maximum particle size. This zone is the primary pathway for sediment routing through or around the pool and can serve to route the coarsest sediment away from the deepest part of the pool. At the tail of the pool, the flow diverges at the head of the riffle leading to deposition on the riffle and the maintenance of a topographic high at the tail of the pool. This hypothesis is consistent with the field measurements and observations of *Keller* [1969], with the simulation results presented in this study, and with other recent studies which have identified flow constrictions as playing a major role in defining pool-riffle morphology.

Acknowledgments

The authors would like to acknowledge Edward Keller for providing access to his unpublished data and field notebooks. The UnTRIM code was provided by Prof. V. Casulli of the University of Trento, Italy. This work was funded in part by a grant from the National Science Foundation (Grant EAR-0087842, Program Manager: Dr. L. Douglas James). Additional funding was provided to MLM by a Stanford Graduate Fellowship and a NSF Graduate Research Fellowship. Financial support for this work was also provided by the US Fish and Wildlife Service (contracting entity for CALFED Bay-Delta Ecosystem Restoration Program: Cooperative Agreement DCN# 113322G003).

References

Bhowmik, N. G., and M. Demissie (1982), Bed material sorting in pools and riffles, *J. Hydraul. Div. Am. Soc. Civ. Engr., 108*, 1227-1231.

Booker, D. J., D. A., Sear, and A. J. Payne (2001), Modeling three-dimensional flow structures and patterns of boundary shear stress in a natural pool-riffle sequence, *Earth Surf. Processes Landforms, 26*, 553-576.

Cao, Z., P. Carling, and R. Oakley (2003), Flow reversal over a natural pool-riffle sequence: a computational study, *Earth Surf. Processes Landforms, 28*, 689-705.

Carling, P. A. (1991), An Appraisal of the Velocity-Reversal Hypothesis for Stable Pool-Riffle Sequences in the River Severn, England, *Earth Surf. Processes Landforms, 16*, 19-31.

Carling, P. A., and N. Wood (1994), Simulation of Flow Over Pool-Riffle Topography: A Consideration of the Velocity Reversal Hypothesis, *Earth Surf. Processes Landforms, 19*, 319-332.

Casulli, V., and P. Zanolli (2002), Semi-implicit numerical modeling of non-hydrostatic free-surface flows for environmental problems, *Mathematical and Computer Modeling, 36*, 1131-1149.

Celik, I., and W. Rodi (1988), Modeling suspended sediment transport in nonequilibrium situations, *J. Hydraul. Engr., 114*(10) 1157-1191.

Clifford, N. J., and K. S. Richards (1992), The Reversal Hypothesis and the Maintenance of Riffle-Pool Sequences: A Review and Field Appraisal, in *Lowland Floodplain Rivers: Geomorphological Perspectives*, edited by P. A. Carling and G. E. Petts, pp. 43-70, John Wiley & Sons, Chichester.

Dietrich, W. E. (1987), Mechanics of flow and sediment transport in river bends, in *River channels: environment and process*, edited by K. Richards, pp. 179-227, Blackwell, Oxford.

Dietrich, W. E., J. D. Smith, and T. Dunne (1979), Flow and sediment transport in a sand bedded meander, *J. Geol., 87*, 305-315.

Froehlich, D. C. (1989), Finite Element Surface-Water Modeling System: Two-Dimensional Flow in a Horizontal Plane-Users Manual, Report FHWA-RD-88-177, pp 285., Federal Highway Administration, Washington D.C..

Keller, E. A. (1969), Form and Fluvial processes of Dry Creek, near Winters, California, M.S. Thesis, University of California, Davis.

Keller, E. A. (1970), Bed-Load Movement Experiments: Dry Creek, California, *J. Sediment. Petrol., 40*, 1339-1344.

Keller, E. A. (1971), Areal Sorting of Bed-Load Material: The Hypothesis of Velocity Reversal, *Geol. Soc. Am. Bull., 82*, 753-756.

Keller, E. A. (1972), Development of alluvial stream channels: a five stage model, *Geol. Soc. Am. Bull., 83,* 1531-1536.

Keller, E. A., and J. L. Florsheim (1993), Velocity-Reversal Hypothesis: A Model Approach, *Earth Surf. Processes Landforms, 18,* 733-740.

Lisle, T. (1979), A sorting mechanism for a riffle-pool sequence, *Geol. Soc. Am. Bull., Part II, 90,* 1142-1157.

MacWilliams, M. L. (2004), Three-dimensional hydrodynamic simulation of river channels and floodplains, Ph.D. Dissertation, 222 pp., Stanford University, Stanford, California.

Miller, A. J. (1994), Debris-fan constrictions and flood hydraulics in river canyons: some implications from two-dimensional flow modelling, *Earth Surf. Processes Landforms, 19*, 681-697.

Pasternack, G. B., C. L. Wang, and J. E. Merz (2004), Application of a 2D hydrodynamic model to design of reach-scale spawning gravel replenishment on the Mokelumne River, California, *River Research and Applications, 20*, 202-225.

Petit, F. (1987), The relationship between shear stress and the shaping of the bed of a pebble-loaded river La Rulles – Ardenne, *Catena, 14*, 453-468.

Petit, F. (1990), Evaluation of grain shear stresses required to initiate movement of particles in natural rivers, *Earth Surf. Processes Landforms, 15*, 135-148.

Richards, K. S. (1978), Simulation of flow geometry in a riffle-pool stream, *Earth Surf. Processes, 3*, 345-354.

Rodi, W. (1993), *Turbulence Models and Their Application in Hydraulics: A state-of-the-art review*, Third Edition, IAHR Monograph Series, A.A. Balkema.

Sear, D. A. (1996), Sediment Transport Processes in Pool-Riffle Sequences, *Earth Surf. Processes Landforms, 21*(3), 241-262.

Shewchuk, J. R. (1996), Triangle: engineering a 2D quality mesh generator and Delaunay triangulator, in *Applied Computational Geometry: Towards Geometric Engineering, vol. 1148*, edited by M. C. Lin and D. Manocha, pp. 203-222, Springer-Verlag.

Thompson, D. M., J. M. Nelson, and E. E. Wohl (1998), Interactions between pool geometry and hydraulics, *Water Resour. Res., 34(12)*, 3673-3681.

Thompson, D. M., E. E. Wohl, and R. D. Jarrett (1996), A revised velocity-reversal and sediment sorting model for a high-gradient, pool-riffle stream, *Physical Geography, 17*(2), 142-156.

Thompson, D. M., E. E. Wohl, and R. D. Jarrett (1999), Velocity reversals and sediment sorting in pools and riffles controlled by channel constrictions, *Geomorphology, 27*, 229-241.

Whiting, P. J., and W. E. Deitrich (1991), Convective accelerations and boundary shear stress over a channel bar, *Water Resour. Res., 27*(5), 783-796.

Table Captions

Table 1: Primary references pertaining to the velocity reversal hypothesis, with our best assessment of the type of study, the parameters evaluated for a reversal, and the authors' support for the velocity reversal and flow-convergence routing hypotheses. For the velocity-reversal hypothesis, stated support indicates that the study supports the velocity reversal hypothesis for the case(s) analyzed; conditional support indicates that the study supported the velocity reversal under some conditions; Inconclusive indicates that no firm statement of support or lack of support was made in the study; negative means the study rejected the hypothesis. For the flow-convergence routing hypothesis, stated support is used for studies that explicitly discuss the significance of either a flow convergence or restriction for the study site(s); implied support applies to studies where these features were noted at the study site but not characterized as an important mechanism.

Figure Captions

Figure 1. Topographic map of a riffle-pool-riffle sequence in Dry Creek near Winters, California (from *Keller and Florsheim* [1993]). Contour interval is 1 ft.

Figure 2. Downstream velocities at pool cross-section predicted using UnTRIM for five flow rates. Cross-sections shown with 2x vertical exaggeration.

Figure 3. Predicted surface velocity vectors and depth on Dry Creek for (a) 0.42 and (b) 17.0 m^3/s flow rates. Surface velocities are shown for a subset of the UnTRIM computational cells.

Figure 4. Predicted and observed near-bottom velocity at pool cross-section for 0.42, 0.97, and 4.5 m^3/s discharges.

Figure 5. Predicted and observed near-bottom velocity at riffle cross-section for 0.42, 0.97, and 4.5 m^3/s discharges.

Figure 6. Mean cross-section velocity as a function of discharge at pool and riffle cross-sections from field measurements [*Keller*, 1969] and predicted using a 1-D model [*Keller and Florsheim*, 1993], 2-D Model (FESWMS) and 3-D model (UnTRIM).

Figure 7. Bed shear stress distribution for four flow rates on pool-riffle sequence on Dry Creek from UnTRIM simulations.

Figure 8. Bed shear stress distribution for four flow rates on pool-riffle sequence on Dry Creek from FESWMS simulations (the modeled reach for the FESWMS simulations was shorter than for the UnTRIM simulations but is shown on the same scale to facilitate comparison).

Figure 9. Bed shear stress as a function of discharge at the pool and riffle cross-sections: (a) Section-average bed shear stress predicted using UnTRIM; (b) Section maximum bed shear stress predicted using UnTRIM; (c) Bed shear stress calculated using the depth-slope product for pool and riffle cross-sections using depth and water surfaces from UnTRIM simulations.

Figure 10. Secondary flow magnitude and direction at pool cross-section A-A' predicted using UnTRIM for five flow rate. Cross-sections shown with 2x vertical exaggeration.

Figure 11. Secondary flow magnitude and direction at riffle cross-section B-B' predicted using UnTRIM for five flow rates. Cross-sections shown with 2x vertical exaggeration.

Figure 12. Downstream velocities at pool cross-section for five flow rates predicted by UnTRIM simulation without advective acceleration. Cross-sections shown with 2x vertical exaggeration.

Figure 13. Conceptual model of flow-convergence routing for pool-riffle sequence on Dry Creek. Depths shown for 4.5 m^3/s discharge.

Figure 14. Lateral sorting of largest bed material size through a pool and adjacent riffle (from *Keller* [1969]). The exact starting points for sediment sampling across the cross-sections are not available, so channel distances are approximate.

Reference	Type of study	Reversal Parameter(s)	Support for Velocity Reversal	Support for Flow Convergence-Routing
Keller [1969]	Field	Near-bed velocity	Stated Support	Implied Support
Keller [1970,1971]	Field	Near-bed velocity	Stated Support	Implied Support
Keller [1972]	Theoretical	N/A	Not Discussed	Stated Support
Richards [1978]	1-D Model	Section-average velocity and shear	Inconclusive	Not Discussed
Lisle [1979]	Field	Mean shear stress	Stated Support	Not Discussed
Bhomik and Demissie [1982]	Field	N/A	Negative	Not Discussed
Petit [1987,1990]	Field	Point shear stress and velocity	Inconclusive	Stated Support
Carling [1991]	Field	Velocity, shear velocity	Negative	Implied Support
Clifford and Richards [1992]	Field	Point and section-averaged velocity and shear stress	Negative	Implied Support
Keller and Florsheim [1993]	1-D Model	Section-average velocity	Stated Support	Not Discussed
Carling and Wood [1994]	1-D Model	Section-average velocity and shear velocity	Conditional Support	Not Discussed
Miller [1994]	2-D Model	N/A	Not Discussed	Stated Support
Sear [1996]	Field, Review	N/A	Negative	Not Discussed
Thompson et al. [1996, 1998, 1999]	Field, Laboratory, 2-D Model	Velocity	Conditional Support	Stated Support
Booker et al. [2001]	3-D Model	Section-average velocity, near-bed velocity, bed shear stress	Conditional Support	Stated Support
Cao et al. [2003]	2-D Model	Bed shear stress, depth-average velocity	Conditional Support	Stated Support

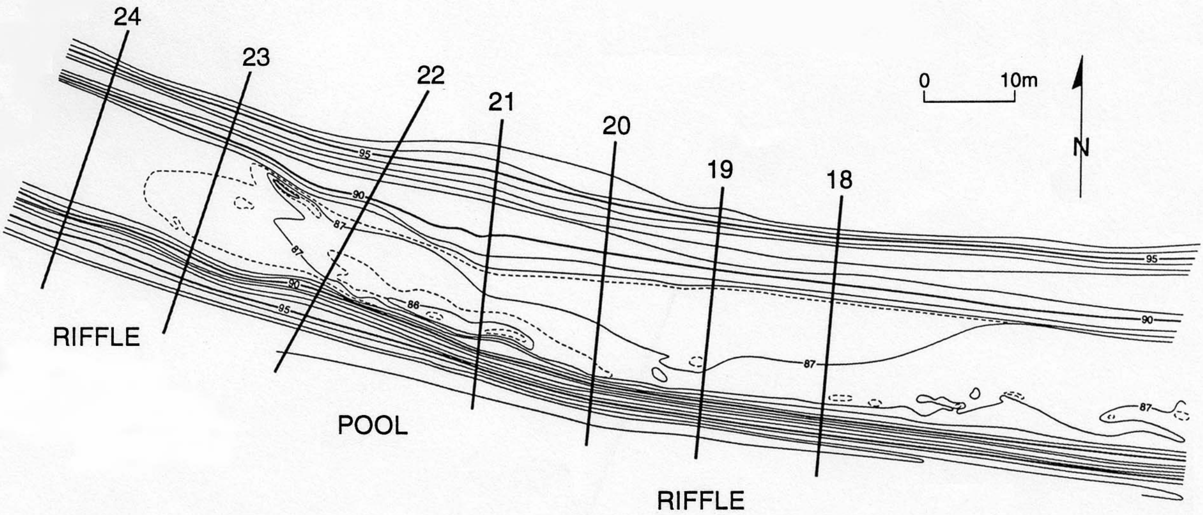
24
23
22
21
20
19
18
0
10m
N
95
90
87
87
90
95
86
87
95
90
87
RIFFLE
POOL
RIFFLE

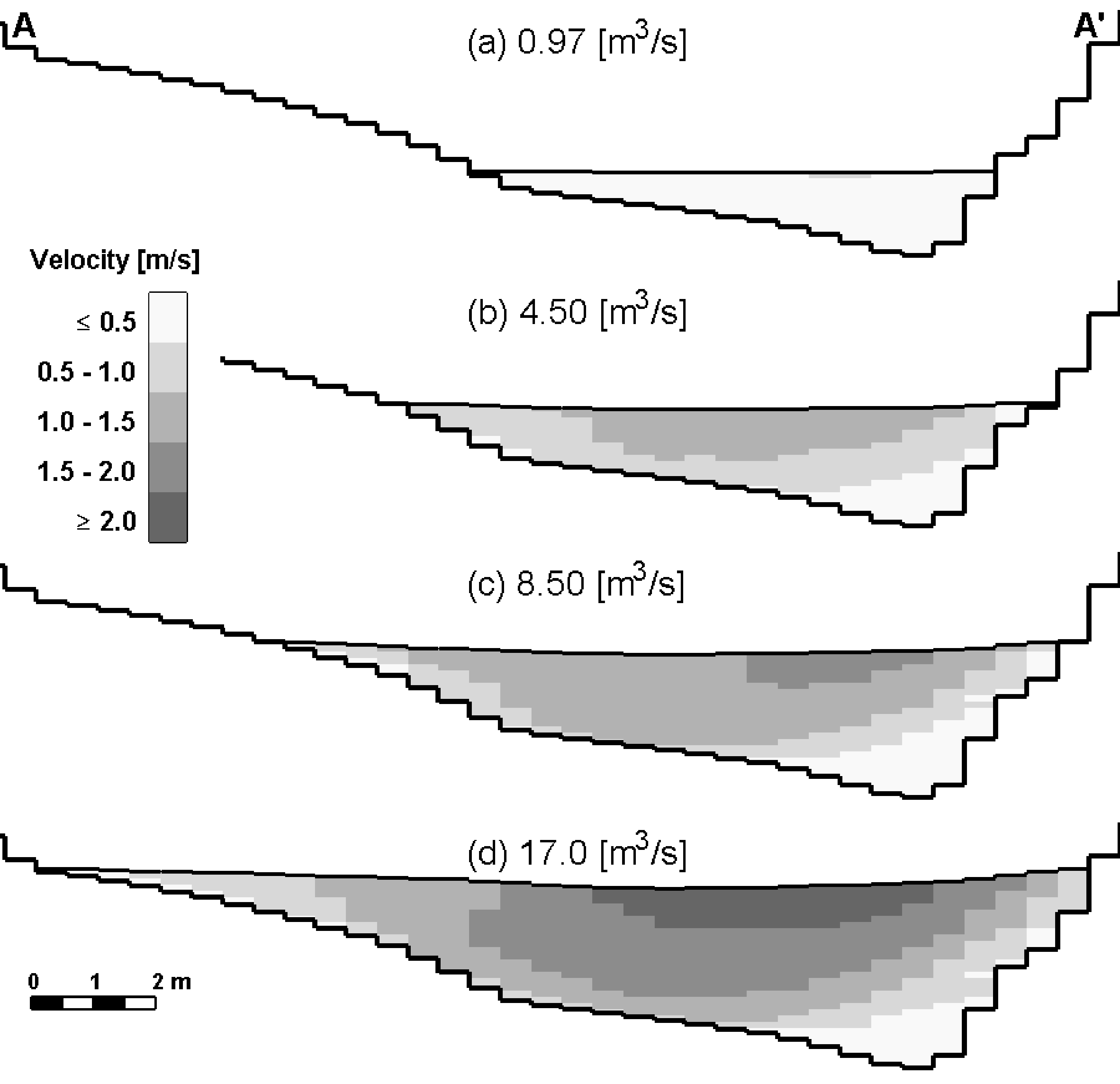

A
A'
(a) 0.97 [m3/s]
Velocity [m/s]
≤ 0.5
0.5 - 1.0
1.0 - 1.5
1.5 - 2.0
≥ 2.0
(b) 4.50 [m3/s]
(c) 8.50 [m3/s]
(d) 17.0 [m3/s]
0
1
2 m

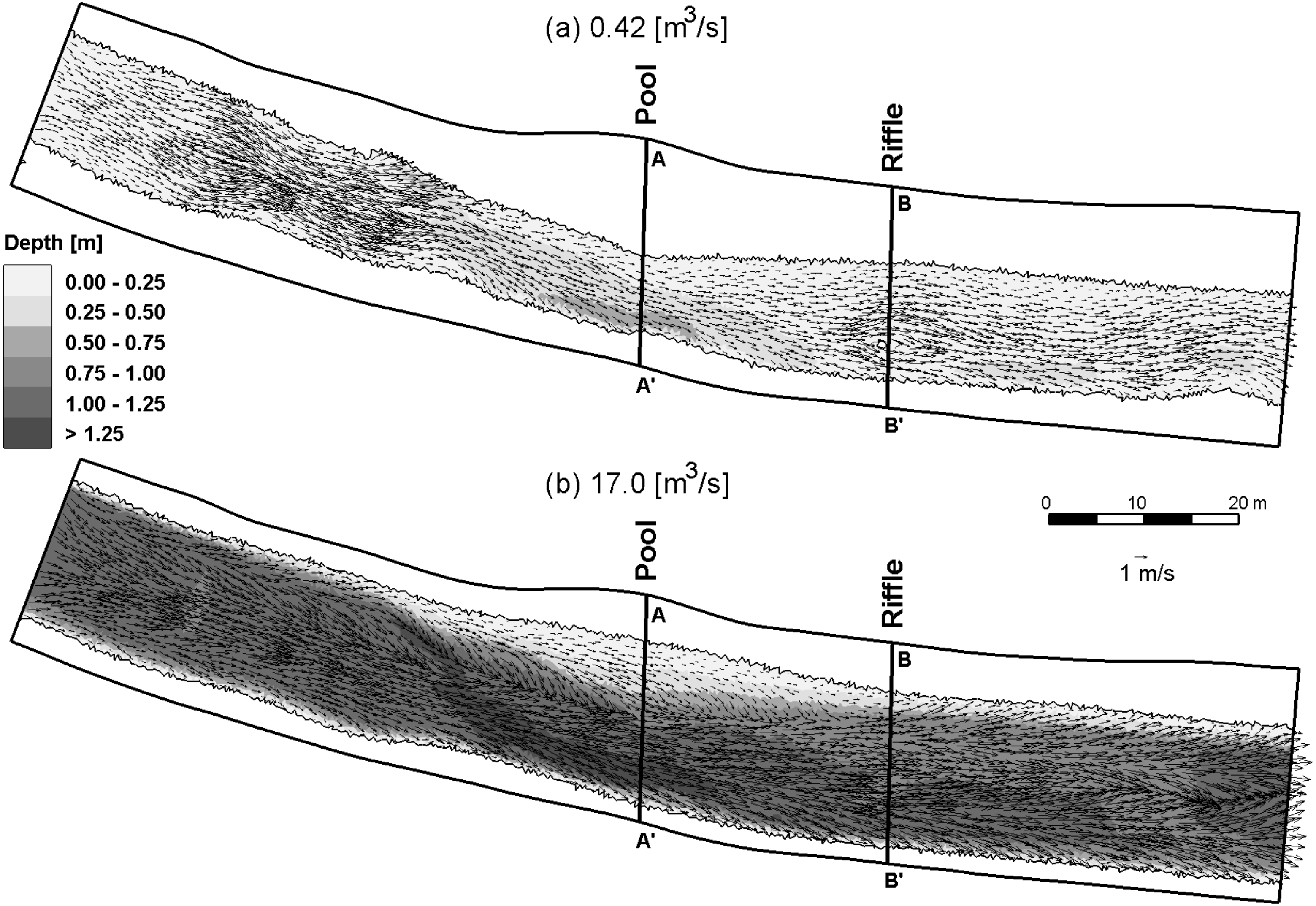

(a) 0.42 [m3/s]
Pool
Riffle
A
A'
B
B'
Depth [m]
0.00 - 0.25
0.25 - 0.50
0.50 - 0.75
0.75 - 1.00
1.00 - 1.25
> 1.25
(b) 17.0 [m3/s]
0
10
20 m
1 m/s
Pool
Riffle
A
A'
B
B'

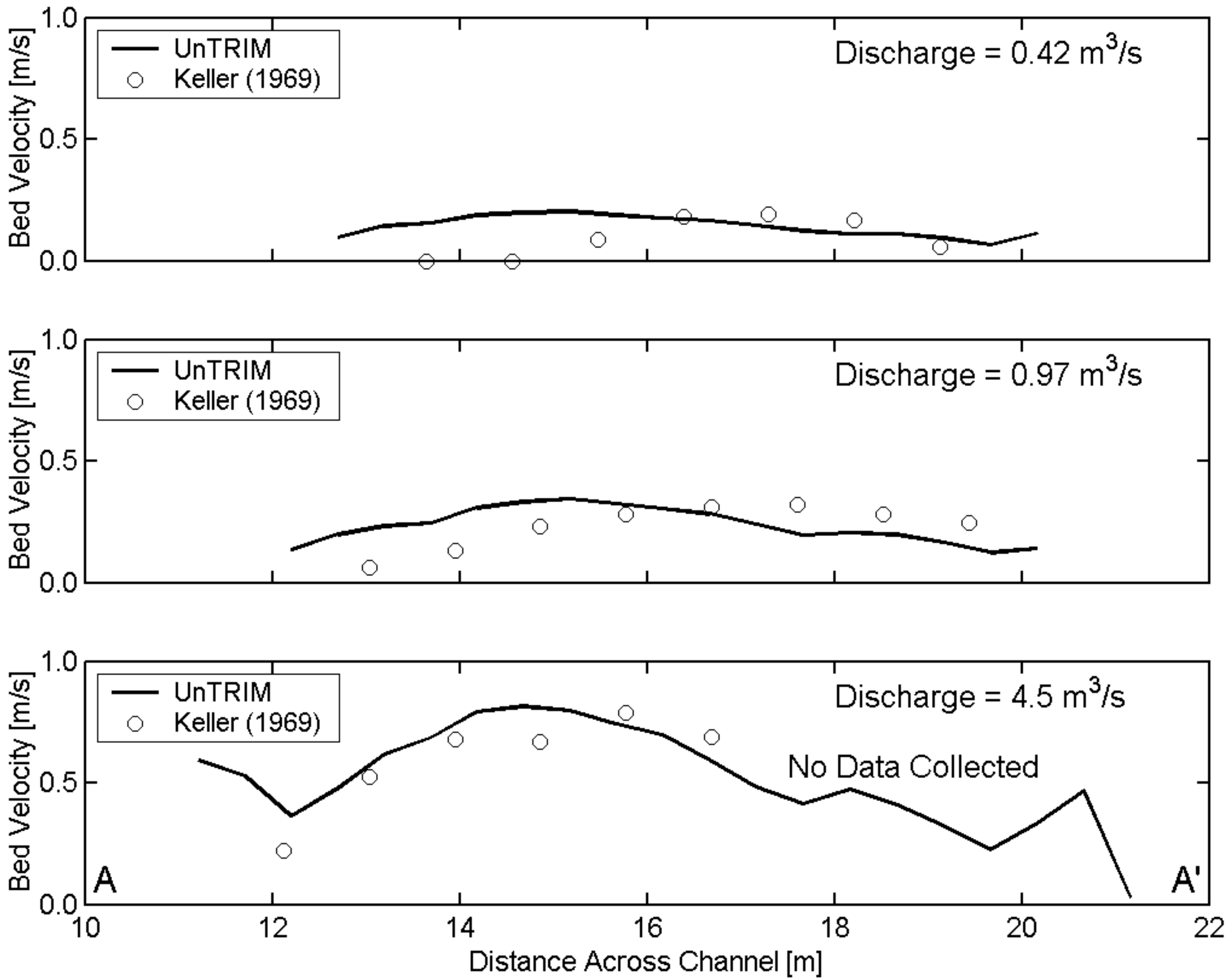

Bed Velocity [m/s]
UnTRIM
Keller (1969)
Discharge = 0.42 m3/s
Discharge = 0.97 m3/s
Discharge = 4.5 m3/s
No Data Collected
A
A'
0.0
0.5
1.0
10
12
14
16
18
20
22
Distance Across Channel [m]

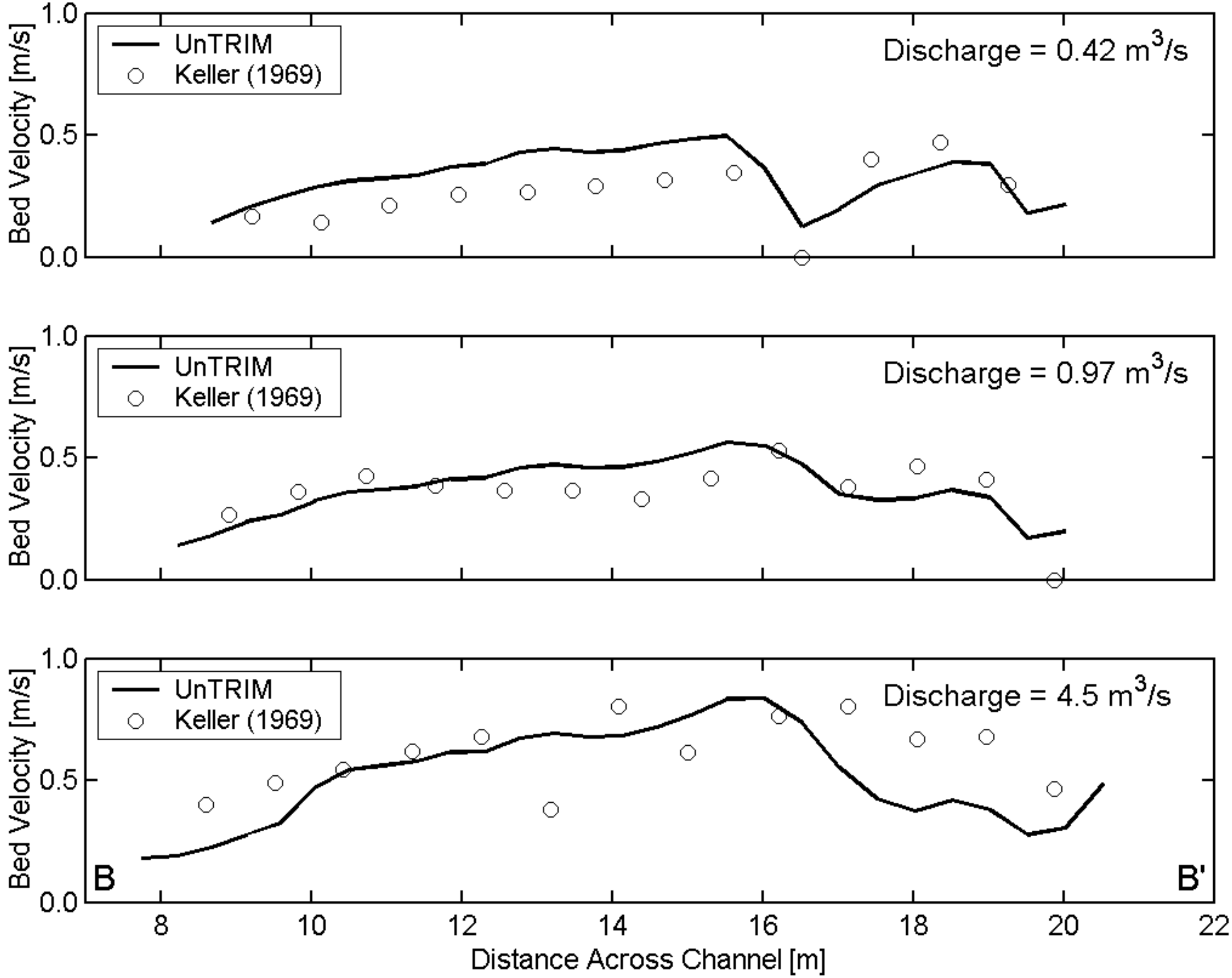

UnTRIM
Keller (1969)
Discharge = 0.42 m3/s
UnTRIM
Keller (1969)
Discharge = 0.97 m3/s
UnTRIM
Keller (1969)
Discharge = 4.5 m3/s
B
B'
Bed Velocity [m/s]
1.0
0.5
0.0
8
10
12
14
16
18
20
22
Distance Across Channel [m]

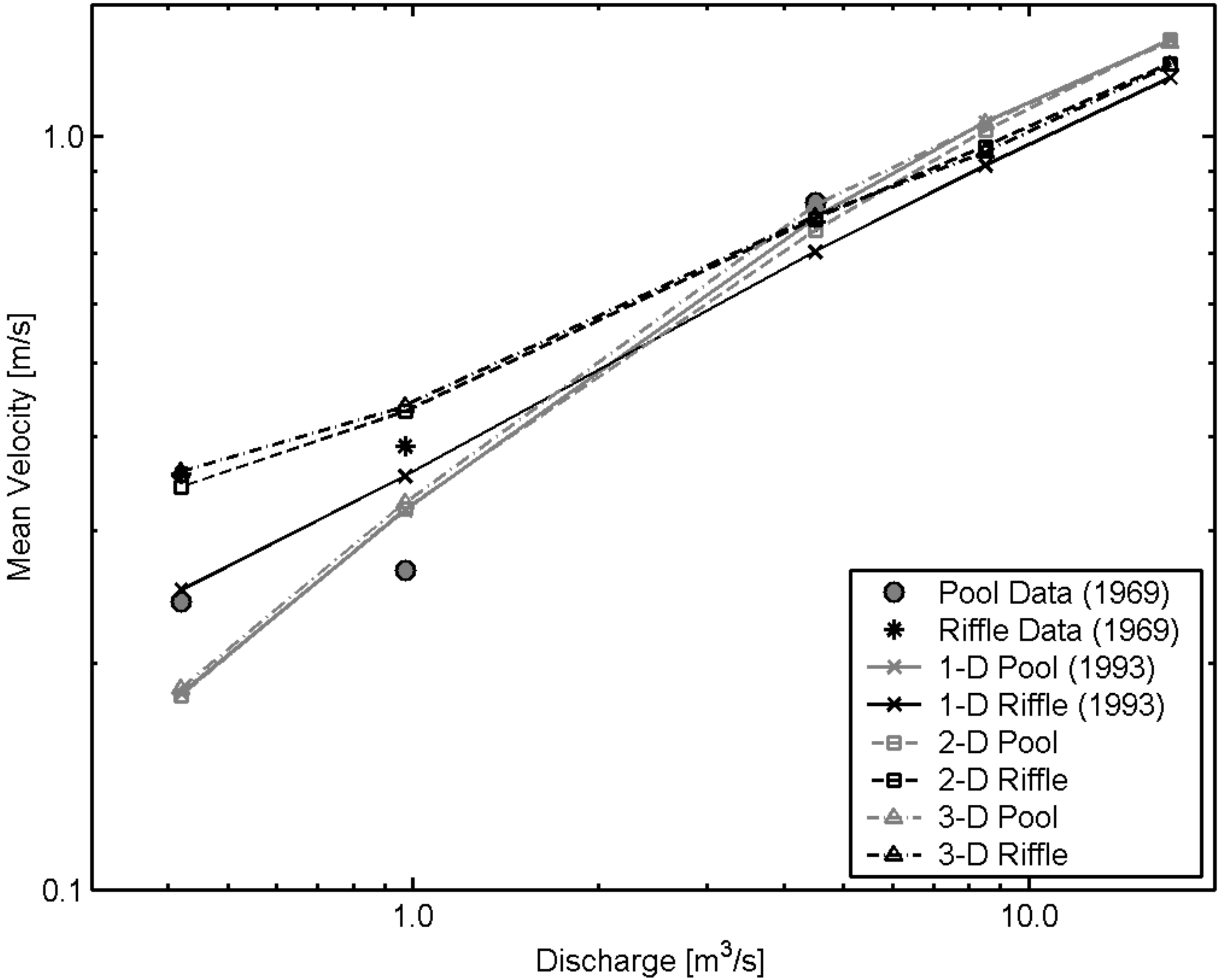

Mean Velocity [m/s]
1.0
0.1
1.0
10.0
Discharge [m^3/s]
Pool Data (1969)
Riffle Data (1969)
1-D Pool (1993)
1-D Riffle (1993)
2-D Pool
2-D Riffle
3-D Pool
3-D Riffle

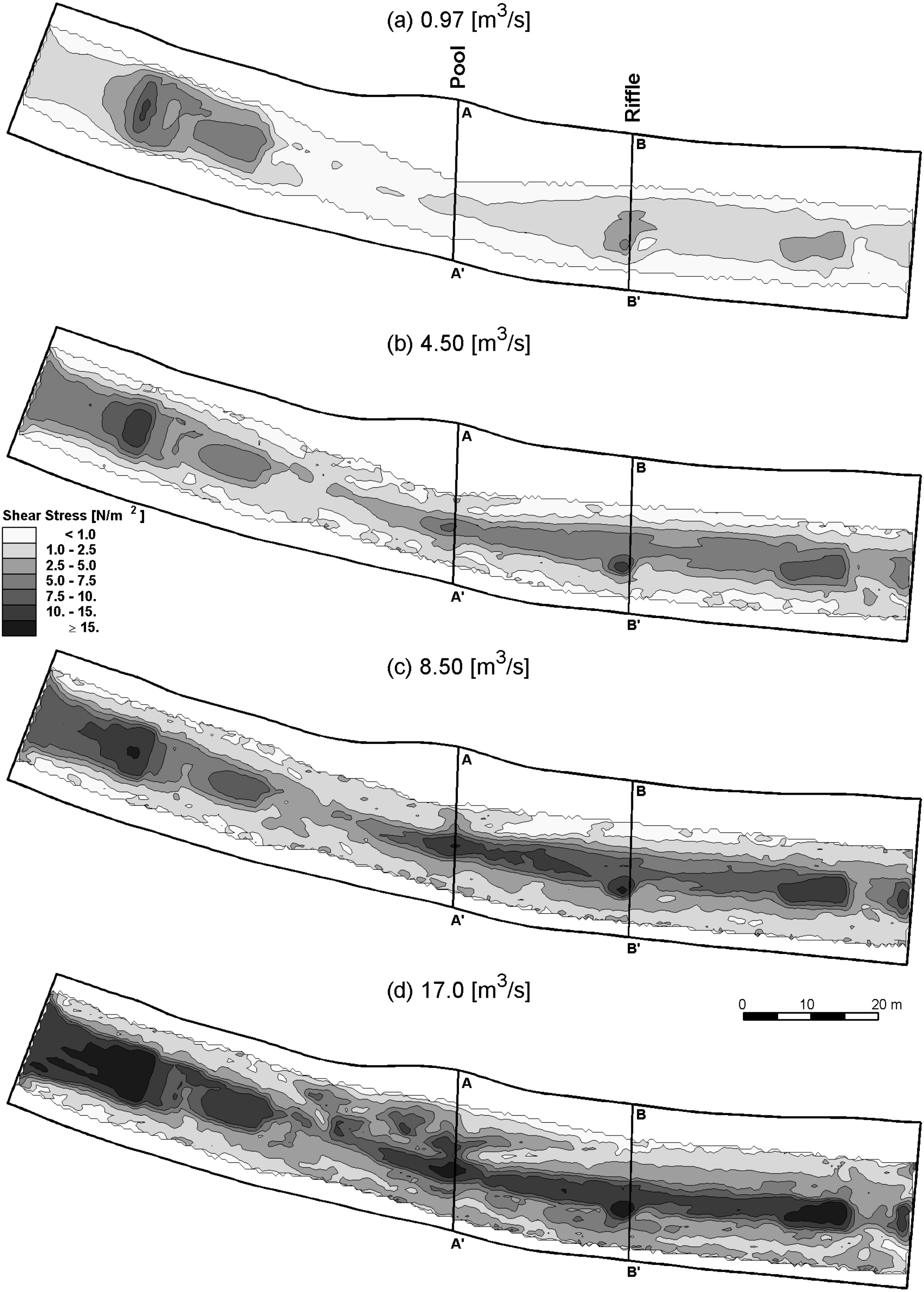

(a) 0.97 [m3/s]
Pool
Riffle
A
A'
B
B'
(b) 4.50 [m3/s]
Shear Stress [N/m 2]
< 1.0
1.0 - 2.5
2.5 - 5.0
5.0 - 7.5
7.5 - 10.
10. - 15.
≥ 15.
(c) 8.50 [m3/s]
(d) 17.0 [m3/s]
0
10
20 m

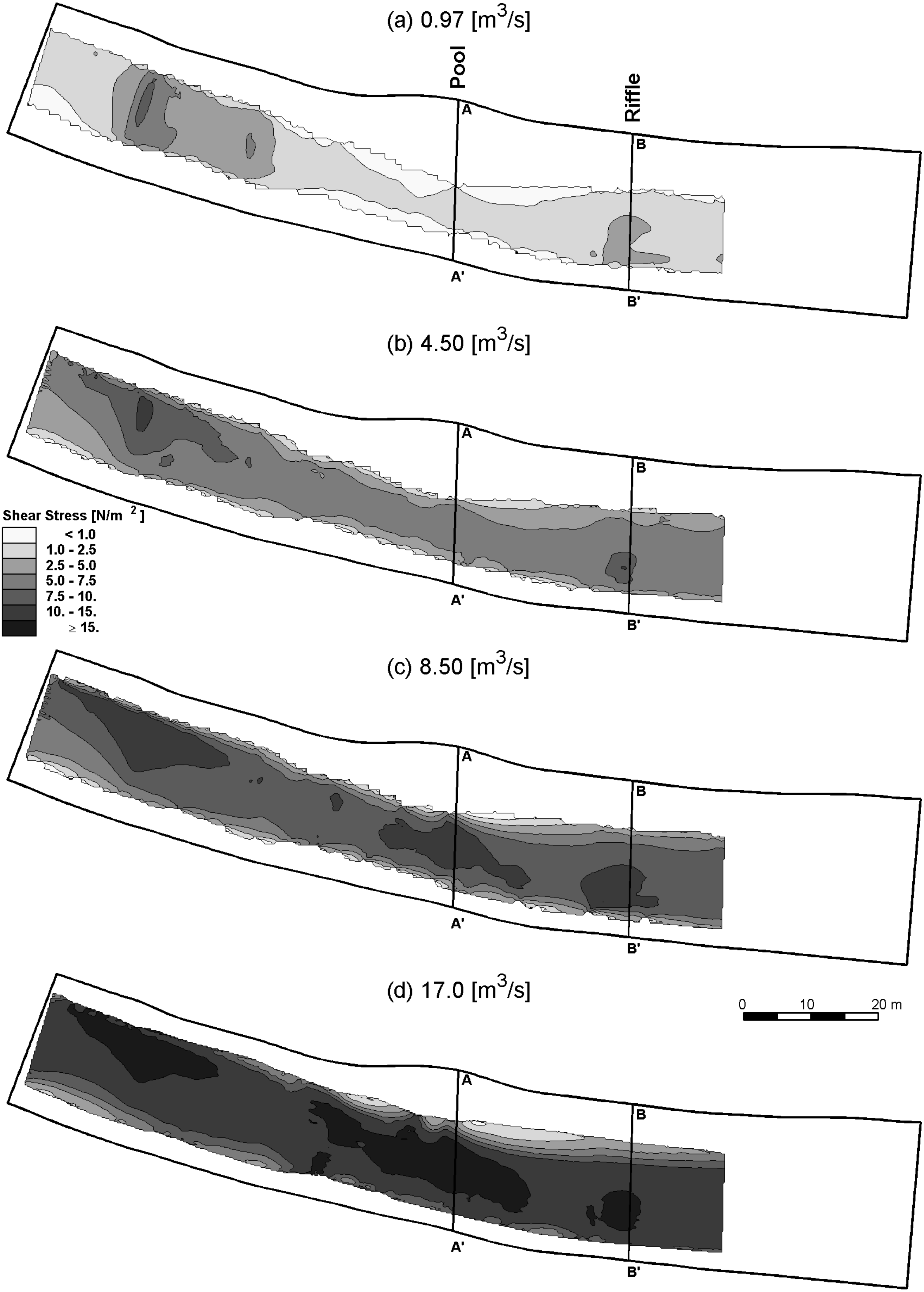

(a) 0.97 [m3/s]
Pool
Riffle
A
A'
B
B'
(b) 4.50 [m3/s]
Shear Stress [N/m 2]
< 1.0
1.0 - 2.5
2.5 - 5.0
5.0 - 7.5
7.5 - 10.
10. - 15.
≥ 15.
(c) 8.50 [m3/s]
(d) 17.0 [m3/s]
0
10
20 m

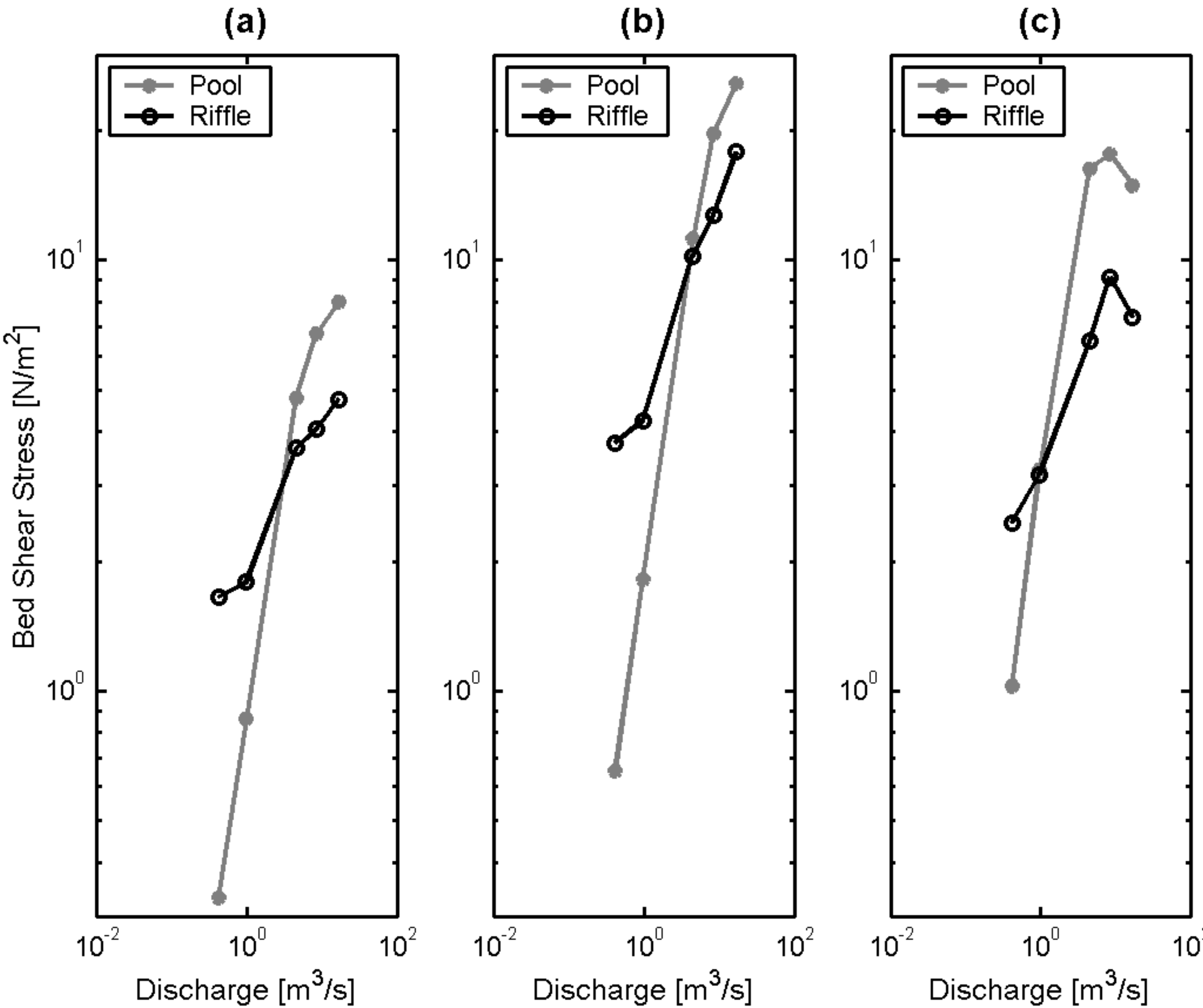

(a)
(b)
(c)
Pool
Riffle
Bed Shear Stress [N/m^2]
10^1
10^0
10^{-2}
10^0
10^2
Discharge [m^3/s]

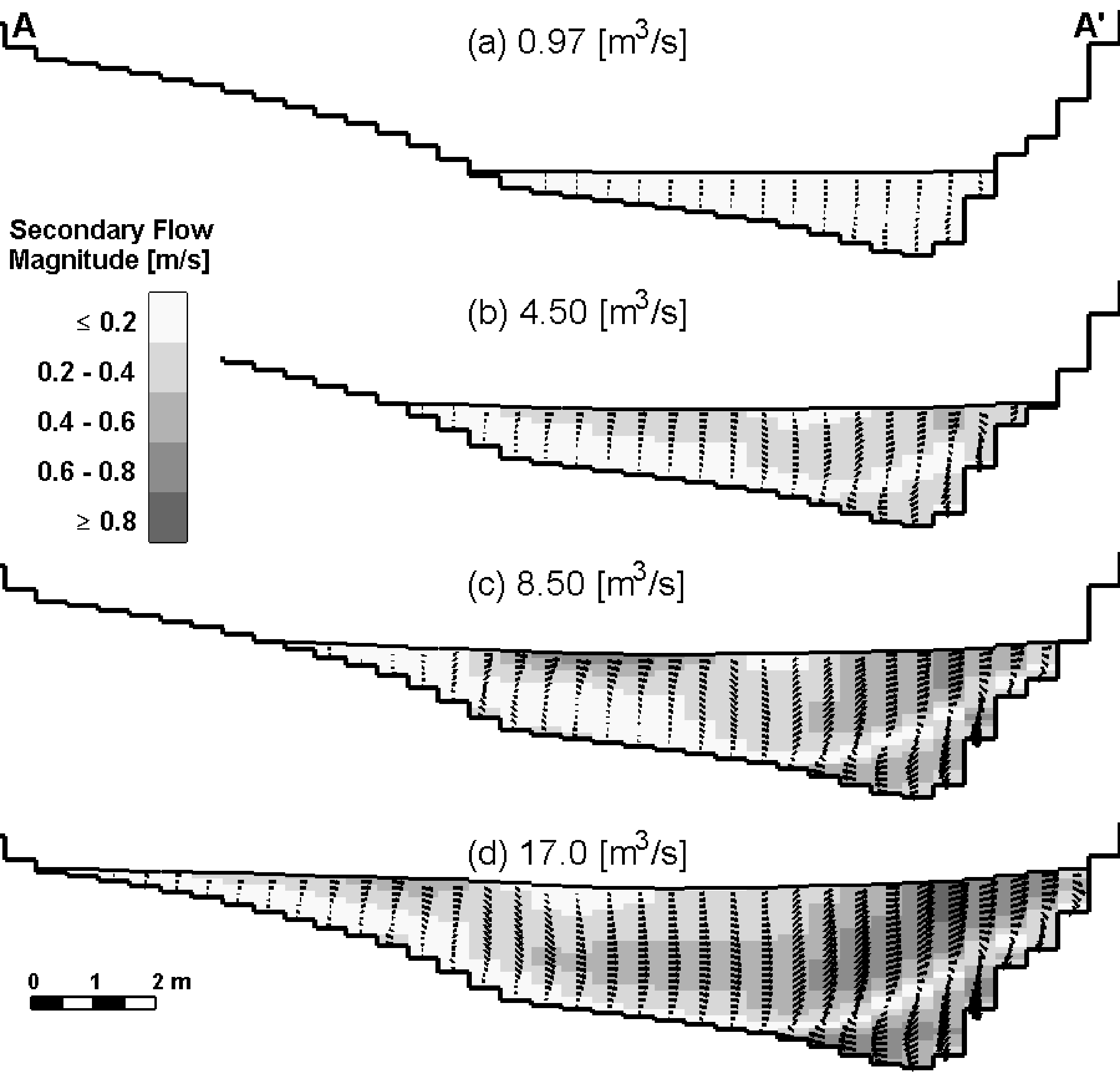
A
A'
(a) 0.97 [m3/s]
(b) 4.50 [m3/s]
(c) 8.50 [m3/s]
(d) 17.0 [m3/s]
Secondary Flow Magnitude [m/s]
≤ 0.2
0.2 - 0.4
0.4 - 0.6
0.6 - 0.8
≥ 0.8
0 1 2 m

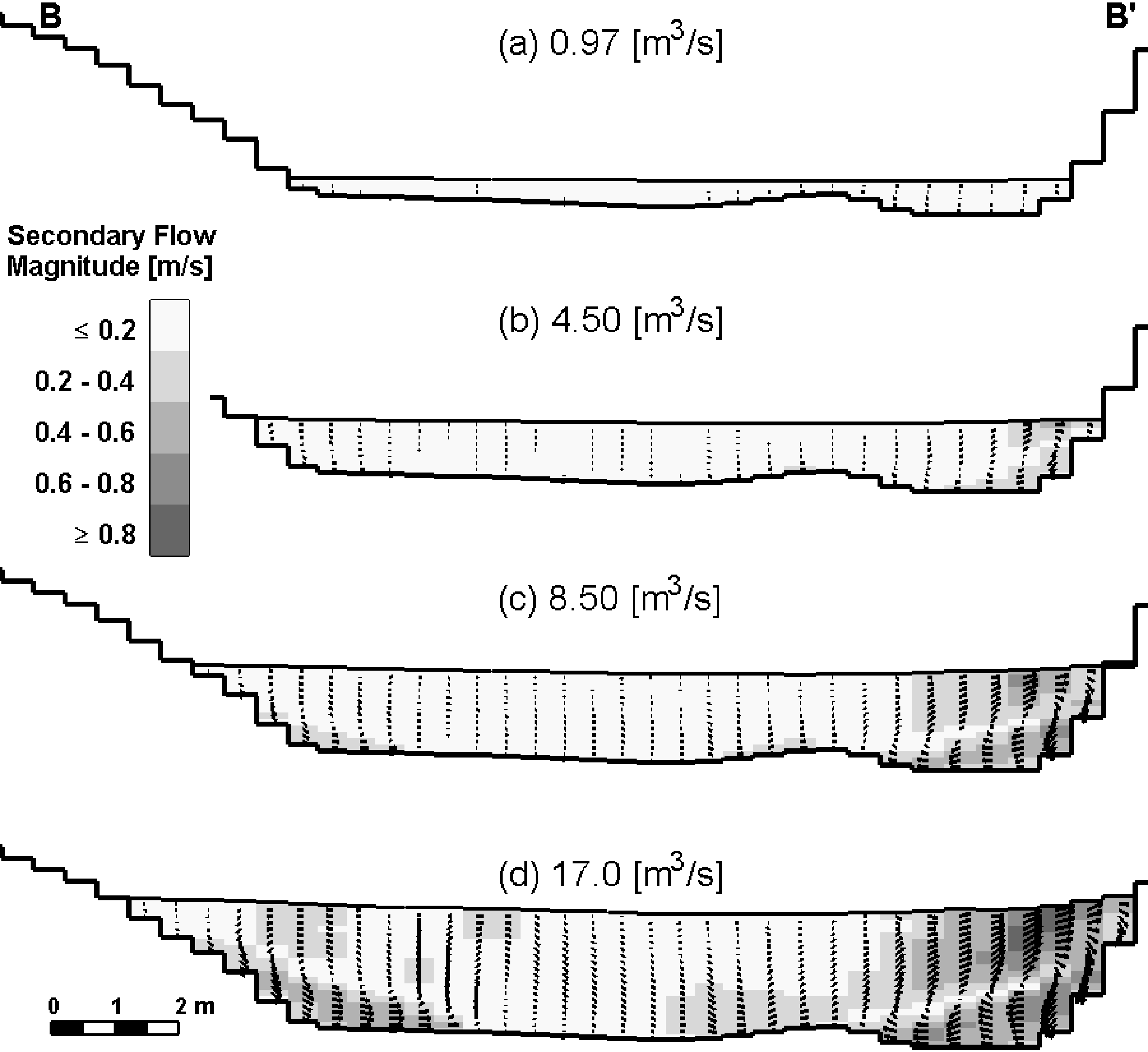
B
B'
(a) 0.97 [m3/s]
Secondary Flow
Magnitude [m/s]
≤ 0.2
0.2 - 0.4
0.4 - 0.6
0.6 - 0.8
≥ 0.8
(b) 4.50 [m3/s]
(c) 8.50 [m3/s]
(d) 17.0 [m3/s]
0
1
2 m

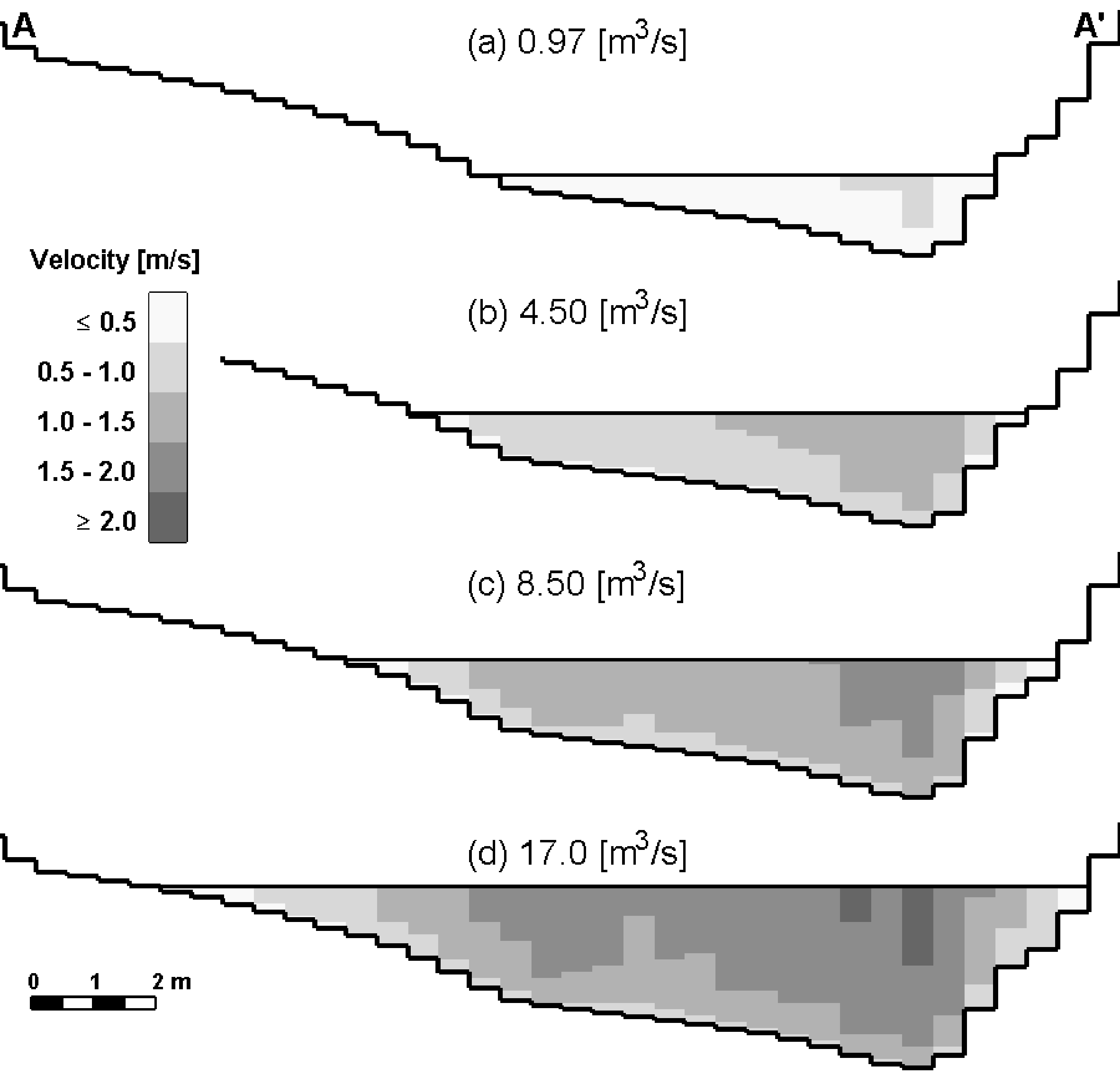
A
A'
(a) 0.97 [m3/s]
Velocity [m/s]
≤ 0.5
0.5 - 1.0
1.0 - 1.5
1.5 - 2.0
≥ 2.0
(b) 4.50 [m3/s]
(c) 8.50 [m3/s]
(d) 17.0 [m3/s]
0
1
2 m

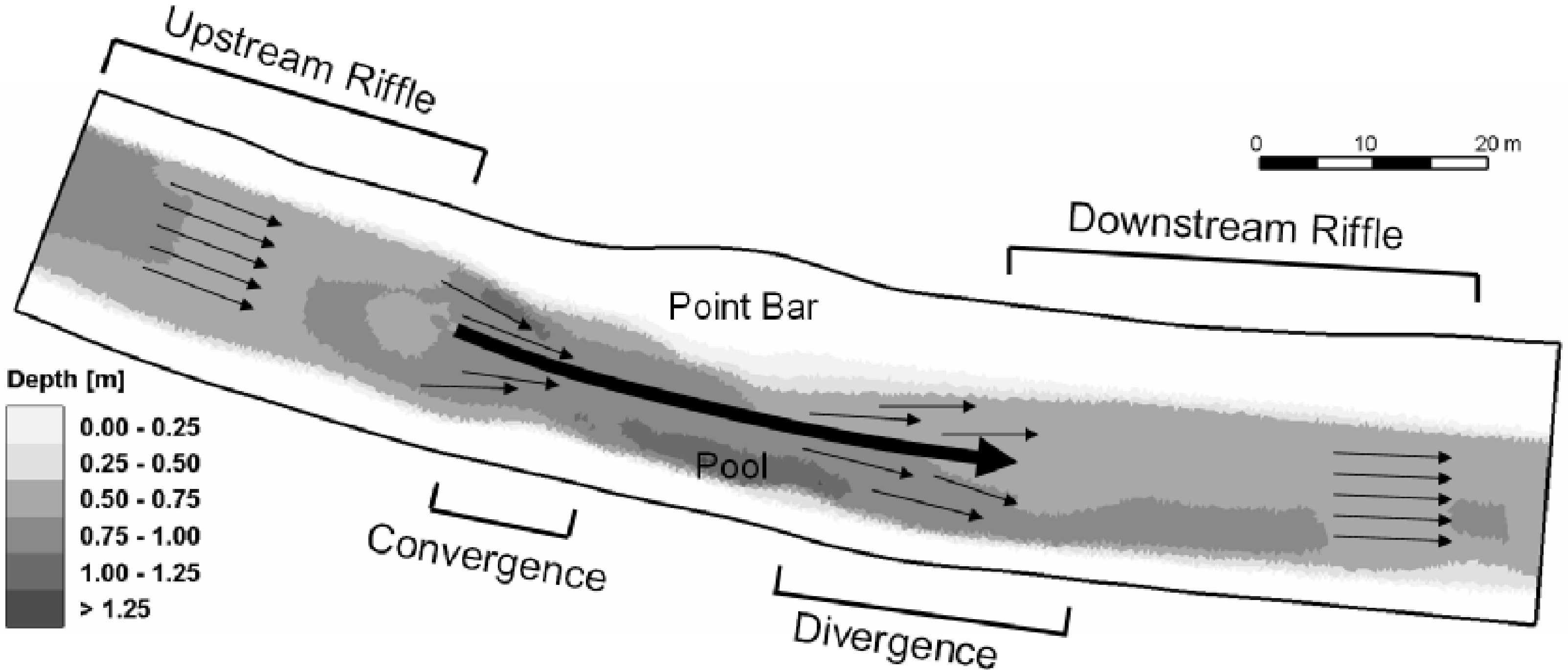
Upstream Riffle
0
10
20 m
Downstream Riffle
Point Bar
Pool
Convergence
Divergence
Depth [m]
0.00 - 0.25
0.25 - 0.50
0.50 - 0.75
0.75 - 1.00
1.00 - 1.25
> 1.25

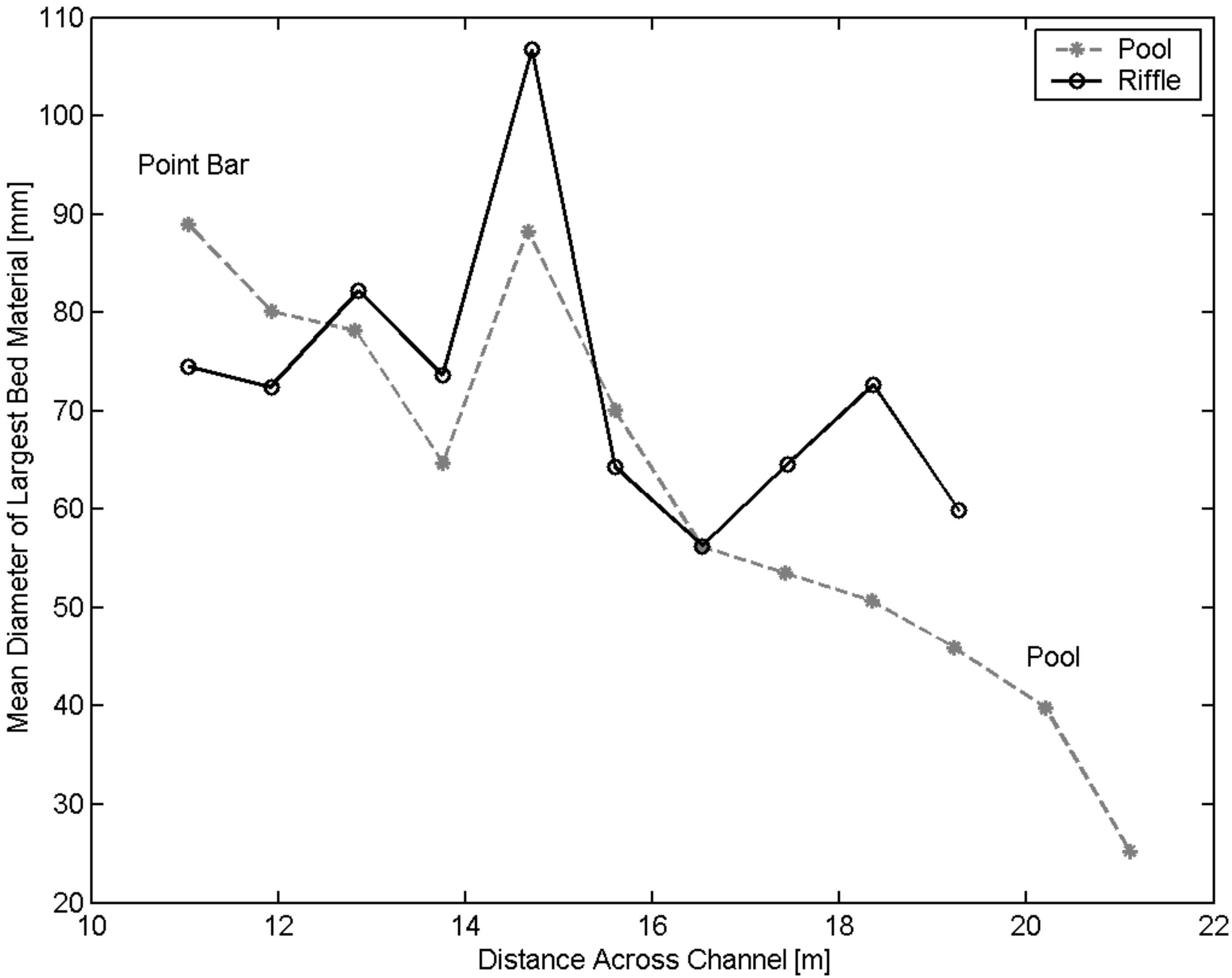

Pool
Riffle
Point Bar
Pool
Mean Diameter of Largest Bed Material [mm]
Distance Across Channel [m]
110
100
90
80
70
60
50
40
30
20
10
12
14
16
18
20
22